Title
Current Clinical Brain Tumor Imaging

Journal
Neurosurgery, 81(3)

ISSN
0148-396X

Authors
Villanueva-Meyer, Javier E
Mabray, Marc C
Cha, Soonmee

Publication Date
2017-09-01

DOI
10.1093/neuros/nyx103

Peer reviewed

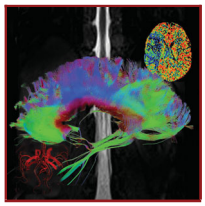

Current Clinical Brain Tumor Imaging

Javier E. Villanueva-Meyer, MD
Marc C. Mabray, MD
Soonmee Cha, MD

Department of Radiology and Biomedical Imaging, Neuroradiology Section, University of California San Francisco, San Francisco, California

Correspondence:
Soonmee Cha, MD,
Department of Radiology and Biomedical Imaging,
University of California San Francisco,
350 Parnassus Ave, Ste 307, Room 307H,
San Francisco, CA 94117.
E-mail: soonmee.cha@ucsf.edu

Received, August 9, 2016.
Accepted, February 23, 2017.
Published Online, May 9, 2017.

Neuroimaging plays an ever evolving role in the diagnosis, treatment planning, and post-therapy assessment of brain tumors. This review provides an overview of current magnetic resonance imaging (MRI) methods routinely employed in the care of the brain tumor patient. Specifically, we focus on advanced techniques including diffusion, perfusion, spectroscopy, tractography, and functional MRI as they pertain to noninvasive characterization of brain tumors and pretreatment evaluation. The utility of both structural and physiological MRI in the post-therapeutic brain evaluation is also reviewed with special attention to the challenges presented by pseudoprogression and pseudoresponse.

KEY WORDS: Brain tumors, Diffusion MRI, Diffusion tensor imaging, fMRI, Neuroimaging, Perfusion MRI, Proton magnetic resonance spectroscopy

Neurosurgery 81:397–415, 2017 DOI:10.1093/neuros/nyx103 www.neurosurgery-online.com

Since the discovery of X-rays more than a century ago, radiology has played an integral role in the diagnosis, monitoring, and treatment planning of intracranial masses. While much progress has been made in both clinical medicine and imaging methodologies since the days of skull radiographs, accurate noninvasive diagnosis and assessment of therapeutic response remain the fundamental goals of imaging in patients with brain tumors. MRI, the mainstay of modern neuroimaging, permits superior structural characterization while also capturing the cellular, vascular, metabolic, and functional properties of brain tumors.

The focus of this review is to provide an overview of the current state of adult brain tumor imaging as it relates to neurosurgical practice. The conventional structural imaging features of brain tumors will be presented and complemented by discussion on advanced imaging methods for surgical planning including perfusion mapping, MR spectroscopy, diffusion tensor imaging, and functional MRI. Lastly, the challenges in post-therapy imaging of brain tumors will be reviewed with specific emphasis on pseudoprogression and pseudoresponse.

CONVENTIONAL MAGNETIC RESONANCE IMAGING FEATURES

Despite the myriad refinements in advanced imaging techniques over the past decades, conventional structural magnetic resonance imaging (MRI) remains the standard of care imaging method for neuro-oncologic practice. Current consensus recommendations for a standardized brain tumor MRI protocol are the following: 3-dimensional (3-D) T1, axial fluid-attenuated inversion recovery (FLAIR), axial diffusion-weighted imaging (DWI), axial gadolinium contrast-enhanced T2, and 3-D gadolinium contrast-enhanced T1, performed on a minimum 1.5 tesla MR system.[1] If 3-D sequences cannot be performed due to time constraints or technical limitations, 2-D

ABBREVIATIONS: ADC, apparent diffusion coefficient; **ASL,** arterial spin labeling; **BBB,** blood–brain barrier; **BOLD,** blood oxygen level dependent; **CNS,** central nervous system; **DCE,** dynamic contrast enhanced; **DMN,** default mode network; **DSC,** dynamic susceptibility contrast; **DTI,** diffusion tensor imaging; **DWI,** diffusion-weighted imaging; **FA,** fractional anisotropy; **FLAIR,** fluid attenuated inversion recovery; **fMRI,** functional MRI; **MD,** mean diffusivity; **MGMT,** O^6-methylguanine DNA methyltransferase; **MRI,** magnetic resonance imaging; **MRS,** MR spectroscopy; **NAA,** *N*-acetylaspartate; **PNET,** primitive neuroectodermal tumor; **PWI,** perfusion-weighted imaging; **RANO,** Response Assessment in Neuro-Oncology; **rCBV,** relative cerebral blood volume; **rs-fMRI,** resting state functional MRI; **RSN,** resting state network; **SMART,** stroke-like migraine attacks after radiation therapy; **SWI,** susceptibility-weighted imaging; **WHO,** World Health Organization; **3-D,** 3-dimensional

TABLE. MRI Techniques and Their Purpose in Brain Tumor Imaging

MRI technique	Clinical utility
T1	Evaluates tissue architecture
	• Precontrast high intensity seen in blood products, mineralization, fat, melanin
	• Postcontrast enhancement reflects nonspecific breakdown of the blood–brain barrier
T2/FLAIR	Evaluates tissue architecture
	• High intensity seen in peritumoral edema (vasogenic and infiltrative), nonenhancing tumor, white matter injury, gliosis
T2* (SWI)	Sensitive to magnetic susceptibility
	• Low intensity seen in blood products, tumoral vascularity, calcification, radiation-induced microhemorrhage
DWI	Probes random motion/diffusion of water, can be presented as ADC map
	• Reduced (high signal intensity) in highly cellular tumor or regions of tumor with increased cellularity and in cytotoxic edema or postoperative injury
MRS	Assesses tumor biochemical/metabolic profile
	• Tumor spectra include elevated Cho, decreased NAA; higher grade glioma show higher Cho/NAA and Cho/Cr ratios than lower grade gliomas
	• Lipid and lactate peaks are not normal and represent necrosis and hypoxia, respectively
Perfusion	DSC—main metric is cerebral blood volume
	• Perfusion curves in gliomas should return close to baseline, perfusion curves in tumors with leaky capillaries (metastases, choroid plexus tumors, extra-axial tumors) generally do not return to baseline
	• Higher blood volume suggests higher grade or progressive/recurrent tumor
	DCE—main metric is the volume transfer constant, a measure of permeability
	• High permeability suggests higher grade and within a tumor may identify regions of higher grade as well or progressive/recurrent tumor
	ASL—main metric is cerebral blood flow
	• Noncontrast technique
	• Higher blood flow can be used for tumor grading or to identify progressive/recurrent tumor
DTI	Analyzes direction of diffusivity and orientation of white matter tracts
	• Tractography demonstrates displacement or infiltration of white matter fiber tracts for surgical planning
fMRI	Assesses brain activation by detecting alterations in blood oxygenation level
	• Task-based fMRI is used for preoperative functional localization
	• Resting-state-fMRI is primarily a research technique

ADC, apparent diffusion coefficient; ASL, arterial spin labeling; Cho, choline; Cr, creatine; DCE, dynamic contrast enhanced; DSC, dynamic susceptibility contrast; DTI, diffusion tensor imaging; DWI, diffusion-weighted imaging; FLAIR, fluid-attenuated inversion recovery; fMRI, functional magnetic resonance imaging; MRS, magnetic resonance spectroscopy; NAA, *N*-acetylaspartate; SWI, susceptibility-weighted imaging

sequences can be substituted. The structural sequences (T2-weighted, FLAIR, and pre- and postcontrast T1-weighted) provide the primary foundation of an MRI examination. Specific presurgical sequences such as high-resolution isovolumetric 3-D T2-weighted and postcontrast 3-D T1 spoiled gradient recalled echo imaging can be obtained with fiducial markers for intraoperative navigation or with a head frame for stereotactic radiosurgical planning.[2-6] In addition to conventional structural sequences, DWI and T2*-weighted imaging, such as susceptibility-weighted imaging (SWI), are usually performed as part of the routine brain MRI examination. An overview of the MRI techniques discussed in this review and their clinical utility is presented in the Table.

Structural MRI

The primary roles of structural MRI in the initial brain tumor evaluation include determining the lesion location, extent of tissue involvement, and resultant mass effect upon the brain, ventricular system, and vasculature.[7] While identifying an accurate histological tumor type can be challenging on the basis of imaging alone, the correct diagnosis can often be suggested in a short list of differential considerations, particularly when imaging features are considered in the context of patient age, symptom duration, presence of extracranial primary malignancy, and history of prior radiation therapy to the brain.

MRI offers superior soft tissue contrast over other cross-sectional imaging techniques allowing for better visualization of subtly infiltrated or disrupted parenchymal architecture. Furthermore, intravenous gadolinium-based contrast agents shorten T1 relaxation times and increase tissue contrast by accentuating areas where contrast agents have leaked out of the blood–brain barrier (BBB) into the interstitial tissues, resulting in parenchymal enhancement. This breakdown of the BBB is a key feature seen in tumors as well as non-neoplastic conditions.[8,9] Within diffuse gliomas, contrast enhancement is positively correlated with tumor grade, although a few high-grade gliomas may show no or minimal enhancement and certain lower grade gliomas (World Health Organization [WHO] grade I) such as pilocytic astrocytoma or ganglioglioma can enhance avidly

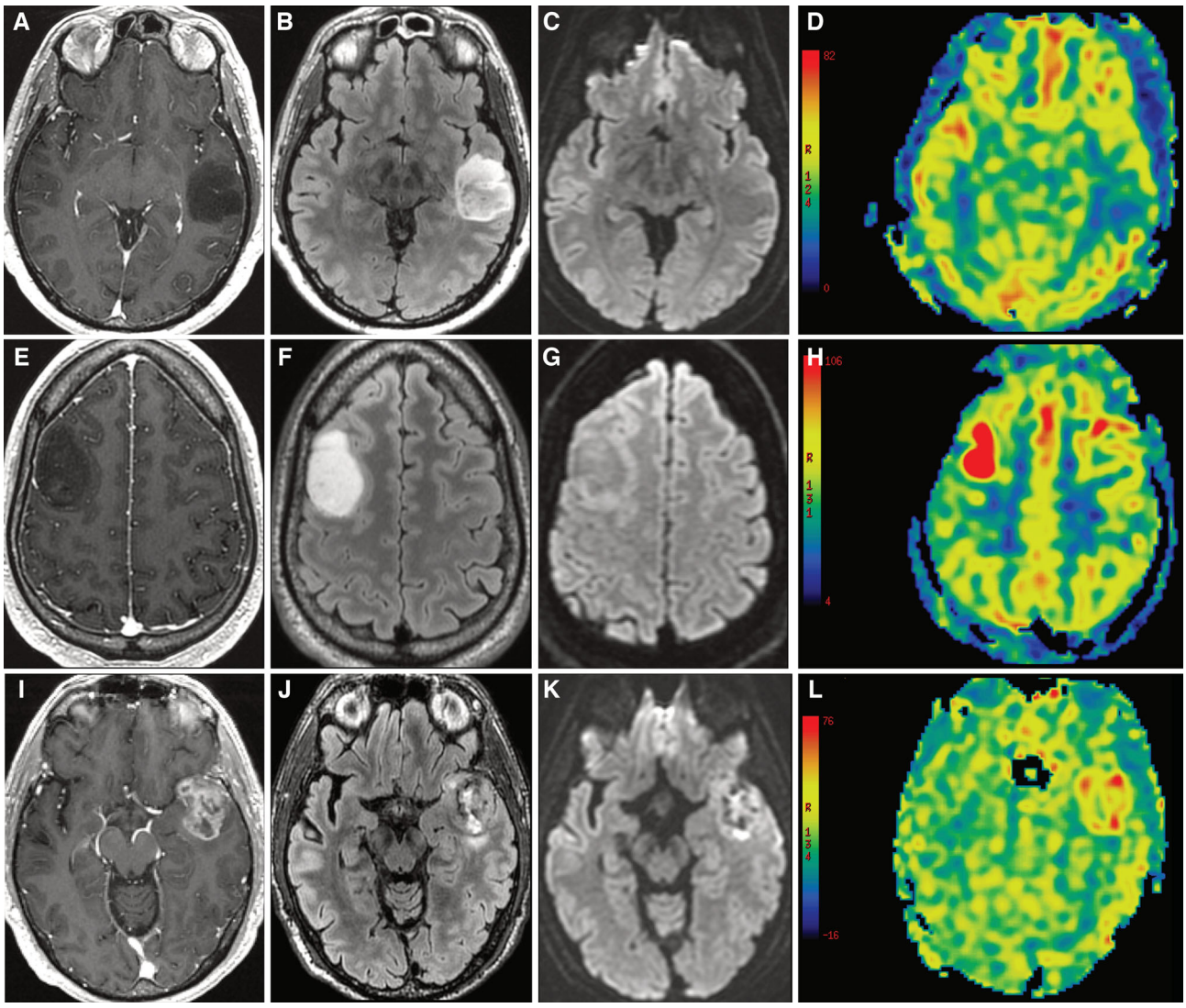

FIGURE 1. *Diffuse astrocytic tumors. Presurgical MRI of 3 patients included axial T1 postcontrast* **A**, **E**, **I**, *axial FLAIR* **B**, **F**, **J**, *axial DWI* **C**, **G**, **K**, *and axial ASL perfusion* **D**, **H**, **L** *sequences. MRI of a 52-yr-old man who presented with headaches and word-finding difficulty shows a left middle temporal nonenhancing* **A**, *FLAIR hyperintense* **B**, *mass without reduced diffusion* **C**, *or elevated cerebral blood flow (*__D__*) found to be a diffuse astrocytoma (WHO grade II). MRI of a 27-yr-old man who presented with seizure shows a right middle frontal faintly enhancing* **E**, *FLAIR hyperintense (*__F__*) mass without reduced diffusion* **G**, *and increased cerebral blood flow (*__H__*) found to be an anaplastic astrocytoma (WHO grade III). MRI of a 76-yr-old man who presented with seizure shows a left anterior temporal heterogeneously enhancing (*__I__*) mass with surrounding FLAIR signal hyperintensity* **J**, *foci of reduced diffusion* **K**, *and elevated cerebral blood flow (*__L__*) found to be a glioblastoma (WHO grade IV).*

(Figure 1).[9] The region of T2/FLAIR hyperintense signal abnormality surrounding the enhancing tumor core is typically referred to as peritumoral edema and can be vasogenic or infiltrative in nature. Vasogenic edema represents a reactive increase in extracellular water due to leakage of plasma fluid from altered tumor capillaries in the absence of tumor cells and is seen around intracranial metastases or noninfiltrative extra-axial tumors such as meningiomas. Infiltrative edema in gliomas represents a mixture of vasogenic edema and infiltrating tumor cells invading along, but not necessarily disrupting, white matter tracts and can be considered nonenhancing tumor owing to preserved integrity of the BBB.[10,11] In fact, in many gliomas, the T2/FLAIR hyperintense signal abnormality may be indistinguishable from the primary mass lesion.[12-14]

Primary lesion location can help differentiate between tumor types. For example, extra-axial tumors such as meningiomas,

schwannomas, and skull base tumors can generally, but not always, be differentiated from intra-axial tumors based on associated interposition of cerebrospinal fluid, vessels, or dura between the mass and cortex.[15] Similarly, the number of lesions is an important consideration as multiple lesions suggest metastatic disease or non-neoplastic processes such as demyelination, inflammation, or infection.[9,16] Finally, several imaging characteristics suggest tumor subtypes. The combination of a cyst and solid nodule within a tumor suggests brain tumors such as gangliglioma, pilocytic astrocytoma, pleomorphic xanthoastrocytoma, and, in the posterior fossa, hemangioblastoma.[17] Calcifications can be seen in oligodendrogliomas, ependymomas, and pineal tumors, among others.[18] Necrosis and hemorrhage are seen with higher grade gliomas, certain metastases, and rarely central nervous system (CNS) lymphoma in immunocompromised patients.[19-21]

Historically, brain tumors have been classified based on histology according to the WHO criteria.[22] Diffuse gliomas are further subdivided into 4 grades by various histological features such as cellularity, nuclear atypia, mitotic activity, pleomorphism, vascular hyperplasia, and necrosis. Grade I gliomas including pilocytic astrocytoma, pleomorphic xanthoastrocytoma, and subependymal giant cell astrocytoma share a relatively benign biology with an indolent clinical course that is distinct from other diffuse infiltrating glioma grades.[23,24] Grade II-IV gliomas are heterogeneous tumors with variable degrees of infiltration, atypia, and mitotic activity. Microvascular proliferation with endothelial hyperplasia and pseudopallisading necrosis are the defining histological hallmarks of grade IV gliomas, frequently referred to as glioblastomas. Recent insights into tumor biology have led to the identification of several molecular aberrations associated with genetic phenotypic differences in brain tumors.[25-31] The updated WHO classification incorporates molecular markers along with histology and defines specific entities on the basis of IDH mutation and 1p19q chromosomal deletion.[32] These, along with other molecular markers including p53, RB1, EGFR, PTEN, MGMT, BRAF, ATRX, TERT, and histone H3, represent a nosological shift where histopathological phenotype is complemented by molecular genetic phenotype to better classify brain tumors and predict their clinical behavior.[33] MRI is rapidly catching up with these genetic advances and helping to noninvasively explore the link between the molecular genetic basis of glioma biology and the imaging characteristics of their morphological phenotypes.

Diffusion-Weighted Imaging

While primarily used in the setting of suspected acute stroke, DWI offers significant value in the evaluation of brain tumors. DWI probes the random (Brownian) motion of water molecules allowing for the assessment of tumor cellularity, peritumoral edema, regions of tumor hypoxia, integrity of white matter tracts, and postoperative injury. Corresponding apparent diffusion coefficient (ADC) values, reflecting the magnitude of diffusivity, are derived for each voxel and displayed as a calculated ADC map.[34-36] Apart from characterizing tumor, DWI can be used to detect non-neoplastic processes such as tumefactive demyelination or infection.[37-39]

In the pretreatment evaluation of brain tumors, DWI best serves to characterize tumor cellularity on the premise that water diffusivity within the extracellular compartment is inversely correlated to the volume of the intracellular space. Low ADC values, representing decreased water diffusivity, can be used to suggest highly cellular tumors such as lymphoma, medulloblastoma, or primitive neuroectodermal tumor (PNET) (Figure 2).[40-42] Additionally, low ADC values can be used as a surrogate for increasing tumor grade or as an independent biomarker signifying poor outcomes both in glioma and lymphoma.[43-45] ADC values have also been used to better localize tumor infiltrated foci among regions of vasogenic edema to better direct tissue sampling and therapy.[46-48] Because of the heterogeneous nature of intracranial tumors, particularly gliomas, histogram analysis can be employed to better assess ADC metrics.[43,49-51] Although some authors have demonstrated good correlation between cell density and ADC values based on stereotactic biopsy, the required postprocessing and overlap in ADC values between tumor grades limit the role of quantitative ADC in clinical practice.

Susceptibility-Weighted Imaging

High-resolution 3-D T2* gradient echo sequences such as SWI are highly sensitive to magnetic susceptibility effects from blood products or mineralization. This technique is useful to depict internal vascular architecture and hemorrhage in tumors, which can be used to suggest grade, as well as calcification, which can be used to narrow the differential diagnosis (Figure 3). Both blood products and mineralization appear dark on magnitude images and can be differentiated on filtered phase images in which paramagnetic blood products appear dark and diamagnetic calcium appears bright (Figure 4).[52,53] Minimum intensity projection images can also be reviewed to more clearly visualize normal venous structures, tumoral vascularity, and parenchymal foci of susceptibility.[54]

PRESURGICAL PLANNING TECHNIQUES

Ongoing challenges in the surgical management of brain tumor patients include selecting an appropriate site for tissue sampling and balancing extent of resection with preservation of eloquent function. In the majority of brain tumors, management focuses on maximal safe resection. However, due to the high variability in eloquent cortex between patients, conventional morphological imaging is not sufficient to predict postsurgical deficits. Advanced MRI techniques, such as perfusion-weighted imaging (PWI), MR spectroscopy (MRS), diffusion tensor imaging (DTI), and functional MRI (fMRI), are used alongside intraoperative cortical mapping to guide the degree of resection for the best clinical outcome.[33,42,55]

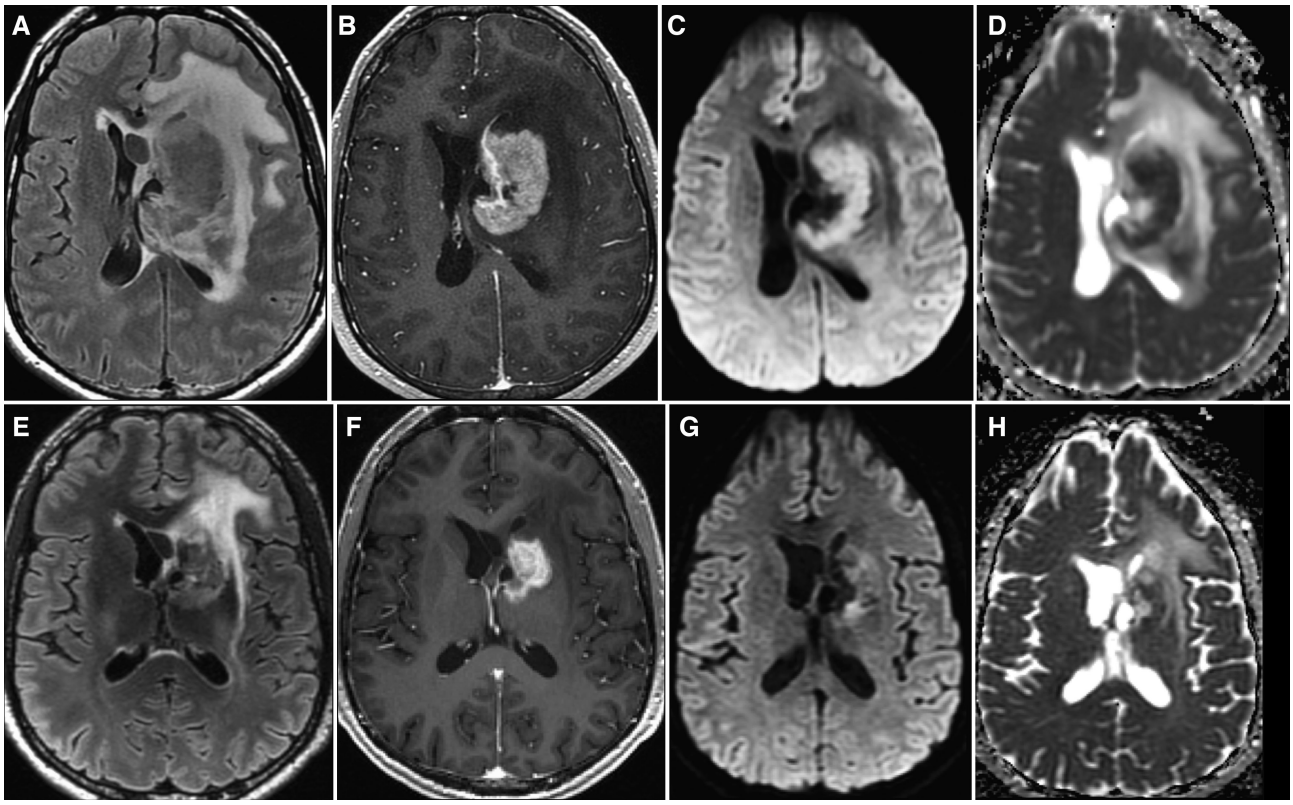

FIGURE 2. *Primary CNS lymphoma. A 33-yr-old woman before (**A**-**D**) and after (**E**-**H**) steroid therapy. Pretreatment MRI shows extensive FLAIR signal abnormality centered in the left basal ganglia and extending throughout the left hemispheric white matter (**A**) as well as contrast enhancement (**B**) associated with reduced diffusion (**C**, DWI; **D**, ADC). MRI obtained 14 days after steroid therapy demonstrates a marked reduction in FLAIR signal abnormality **E**, contrast enhancement **F**, and reduced diffusion (**G**, DWI; **H**, ADC).*

MR Perfusion Imaging

Several MR perfusion techniques are currently employed: dynamic susceptibility contrast (DSC), dynamic contrast-enhanced (DCE), and arterial spin labeling (ASL). Of these, DSC perfusion is the most studied and widely applied, while ASL, which does not require intravenous contrast, has been the subject of increasing investigation and clinical implementation.[56,57]

DSC is based on the detection of susceptibility induced signal loss on T2*-weighted sequences after the administration of an intravenous gadolinium contrast agent. A signal intensity time curve is generated from which relative cerebral blood volume (rCBV) and other perfusion metrics are derived. rCBV is elevated in tumor, where it is seen as a marker of angiogenesis, and has been shown to distinguish tumor from non-neoplastic etiologies with lower rCBV such as demyelinating lesions. A signal intensity time curve that does not return to baseline is seen with leaky capillaries and can suggest metastasis, meningioma, or choroid plexus tumor.[57] rCBV has been positively correlated to glioma grade, although some lower grade gliomas such as oligodendrogliomas may have elevated rCBV.[44,58] rCBV has been noted to be increased in infiltrative edema of gliomas compared to acellular vasogenic edema surrounding metastases, a characteristic which may be used to better target biopsy.[59] rCBV may also predict areas of progression in glioma prior to changes on contrast-enhanced MRI as well as survival.[60]

The underlying principle behind DCE is that disordered tumor vasculature permits intravascular contrast diffusion into the interstitial compartment which is then quantifiable over a dynamic MR acquisition. The volume transfer constant or k^{trans}, a measure of capillary permeability, is the primary metric derived from DCE perfusion. k^{trans} can be used to grade tumors, particularly gliomas, as gliomas with increased capillary permeability are more likely to be higher grade than lower grade. Another metric quantified by DCE is v_e, an estimate of fractional extracellular extravascular space, which has been shown to be related to tumor cellularity, though a strong relationship has not clearly been established.[61-65] Currently, DCE has not gained widespread clinical use because of challenges in acquisition and analysis techniques.

ASL is a noninvasive perfusion imaging technique which quantitatively measures cerebral blood flow. It uses an inversion

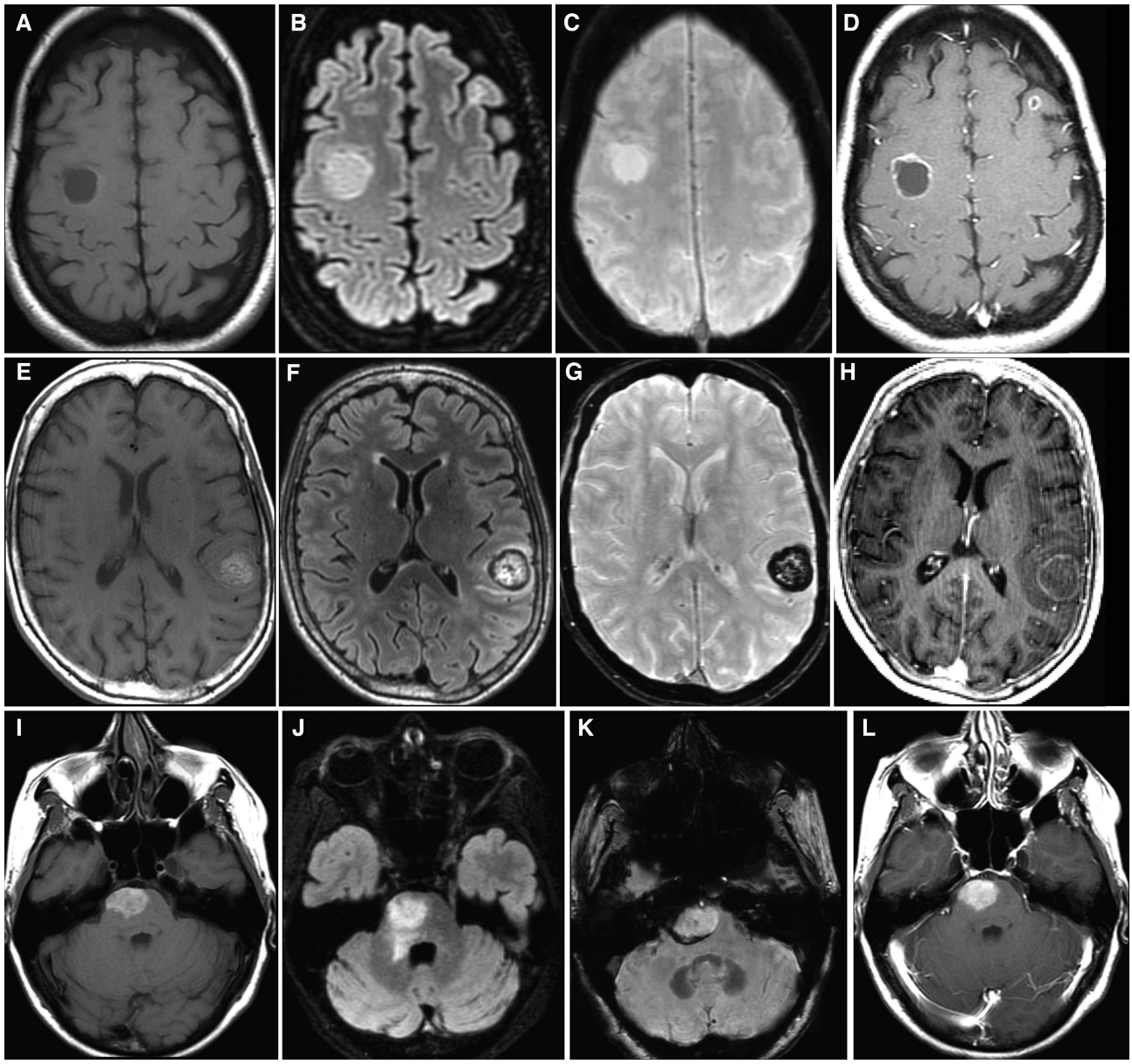

FIGURE 3. *Intracranial metastases. Pretreatment MRI of 3 patients included axial T1 precontrast* **A**, **E**, **I**, *axial FLAIR* **B**, **F**, **J**, *axial SWI* **C**, **G**, **K**, *and axial T1 postcontrast* **D**, **H**, **L** *sequences. MRI of a 50-yr-old woman with breast cancer shows bilateral frontal T1 hypointense (***A***) masses with surrounding edema* **B**, *without susceptibility* **C**, *and with peripheral enhancement (***D***) consistent with multiple nonhemorrhagic metastases. MRI of a 63-yr-old man with lung cancer shows a left parietal mass with intrinsic T1 signal hyperintensity* **E**, *minimal surrounding edema* **F**, *susceptibility on SWI* **G**, *with peripheral enhancement (***H***) consistent with a hemorrhagic metastasis. Given the susceptibility on SWI, the intrinsic high T1 signal represents blood products in this case. MRI of a 58-yr-old woman with melanoma shows a ventral pontine mass with intrinsic T1 signal hyperintensity* **I**, *minimal edema* **J**, *minimal peripheral susceptibility* **K**, *and no significant enhancement (***L***) consistent with a melanoma metastasis. Given the relative lack of susceptibility on SWI, the intrinsic high T1 signal represents melanin in this case.*

pulse to label inflowing blood proximal to the area of imaging with subsequent subtraction of these labeled spins from control static images. ASL is of particular clinical interest due to its noncontrast technique, relative speed, ability to image the whole brain, and minimal postprocessing.[66,67] Several studies have shown a promising role for ASL in quantitative characterization of tumor vascularity in meningioma, metastasis, and high-grade glioma as well as in its ability to differentiate high- from

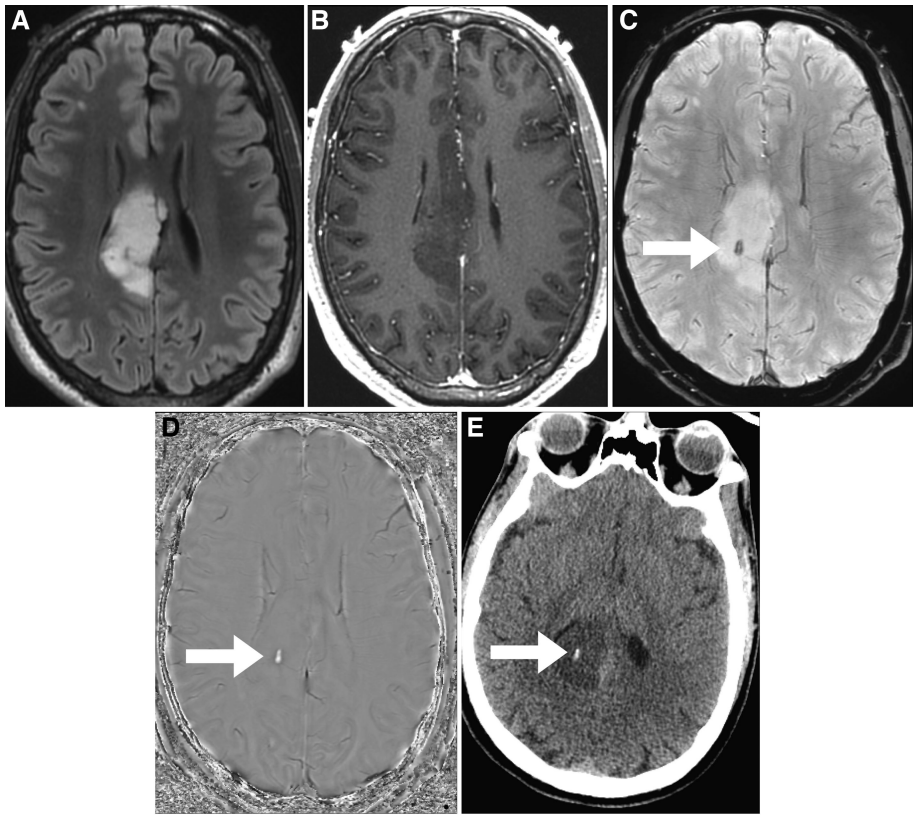

FIGURE 4. *SWI in oligodendroglioma. A 40-yr-old man who presented with loss of consciousness. Presurgical imaging included axial FLAIR* **A**, *axial T1 postcontrast* **B**, *axial SWI* **C**, *and SWI phase (***D***) sequences as well as axial noncontrast CT* **E**. *MRI demonstrates a FLAIR hyperintense* **A**, *nonenhancing* **B**, *infiltrative mass within the right cingulate gyrus found to represent an oligodendroglioma. A punctate focus of susceptibility (C; white arrow) with high signal intensity on filtered phase images (***D***; white arrow) corresponds to calcification on CT (***E***; white arrow).*

low-grade gliomas based on a degree of microvascular proliferation (Figure 1).[68-72]

MR Spectroscopy

MRS provides insight into the biochemical profile of interrogated brain tissue. Proton (^{1}H) MRS is the most studied technique and can be performed with long (288 or 144 ms) and short (35 ms) echo times. MRS can be obtained using a single-voxel technique to a targeted region of interest or a multivoxel technique to cover a broader area and better evaluate regional biochemical differences. The most recognizable metabolite peaks on long echo ^{1}H MRS include *N*-acetylaspartate (NAA) at 2.0 parts per million (ppm), creatine (Cr) at 3.0 ppm, choline (Cho) at 3.2 ppm, and myo-inositol (MI) at 3.5 ppm. NAA is a marker of neuronal viability, Cr reflects normal cellular metabolism, Cho is a marker of cell membrane turnover, and MI reflects astrocyte integrity. Lipid and lactate, which have a broad peak at 1.3 ppm, are not seen in normal tissue and considered markers of necrosis and hypoxia, respectively. A normal spectrum demonstrates upward sloping of peaks from myo-inositol to choline, forming the so-called Hunter's angle of approximately 45°.[73-75]

Brain tumor spectra reflect cellular turnover and loss of normal neuronal metabolites, typically as elevated Cho and decreased NAA resulting in a downward sloping appearance of metabolite peaks or reversal of the usual Hunter's angle.[75] Generally, absolute heights of metabolite peaks are not used, and rather the peaks are analyzed as ratios such as Cho/NAA and Cho/Cr.[74,76] MRS has been shown to differentiate gliomas by grade on the basis of a positive correlation between Cho/NAA and Cho/Cr ratios and grade.[77-80] Additionally, lower grade gliomas have been associated with elevated MI/Cr ratio.[81] Within regions of nonenhancing signal abnormality, elevated Cho/NAA and Cho/Cr ratios have been observed in infiltrative edema compared to vasogenic edema reflecting the increased cellularity underlying the signal abnormality (Figure 5). In this way, MRS can be used to differentiate glioma from noninfiltrative tumor such as metastasis or for biopsy targeting and treatment planning in glioma.[82-86]

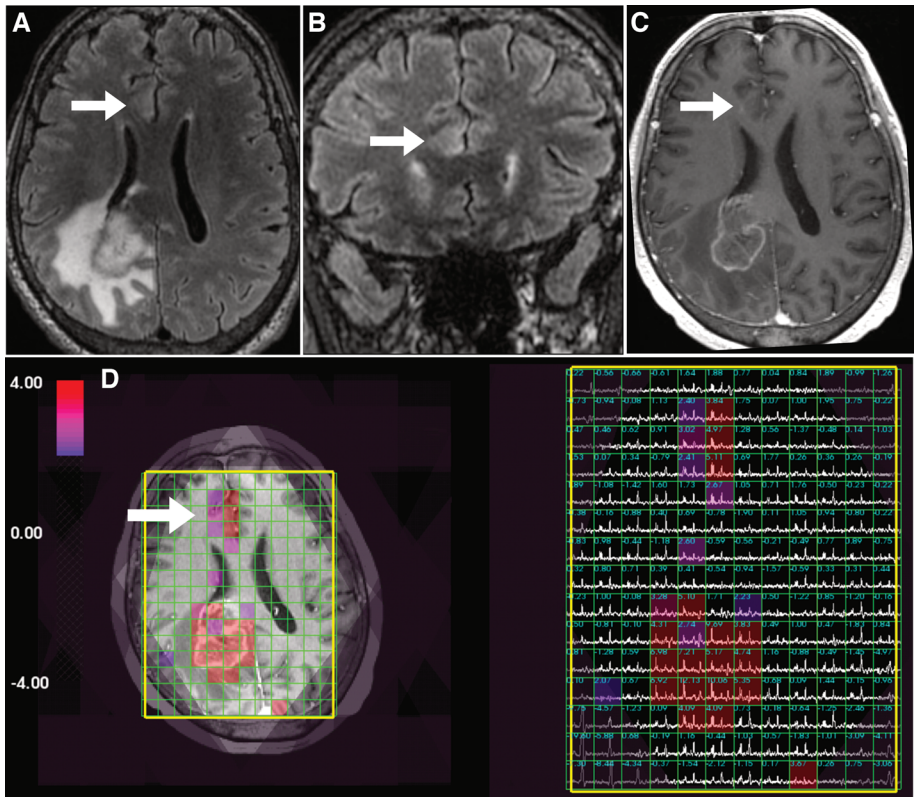

FIGURE 5. *MRS in glioblastoma. A 65-yr-old man with glioblastoma. Presurgical MRI included axial FLAIR* **A**, *coronal FLAIR* **B**, *and axial T1 postcontrast (***C***) sequences as well as multivoxel spectroscopy with Cho/NAA ratios overlaid on T1 postcontrast images* **D**. *A dominant, peripherally enhancing (***C***) right parietal mass with surrounding edema (***A***) shows an elevated Cho/NAA ratio* **D**. *Another subtle focus of FLAIR signal hyperintensity* **A**, **B**; *(white arrows) with minimal enhancement* **C** *is also shown to have an abnormally elevated Cho/NAA ratio (***D**, *white arrow) consistent with multifocal glioma.*

Widespread adoption of MRS is limited by technical issues such as variability in acquisition techniques, differences in metabolite ratio calculations, and volume averaging due to lesion location or voxel size. Despite these challenges, MRS is able to add specificity to conventional MRI and remains an area of intense investigation that, with further refinements, will see increased clinical adoption.

Diffusion Tensor Imaging

An advanced application of diffusion imaging is DTI, which interrogates the 3-D shape of diffusion using both diffusivity (eigenvalues) and direction (eigenvectors). The principle metrics obtained from DTI include mean diffusivity (MD) and fractional anisotropy (FA). In presurgical planning, DTI-based tractography is used to guide surgical resection by analyzing the integrity of white matter fiber trajectory in order to determine whether there is tumor invasion or tumor displacement of the adjacent white matter tracts (Figures 6 and 7).[87,88]

FA represents the degree of directionality of water diffusion and in the normal brain reflects the presence of intact myelinated white matter tracts. In brain tumors, disrupted cellular architecture results in altered FA that correlates to cellularity.[69] Longer progression-free survival and overall survival were seen in glioblastoma patients in whom more DTI abnormality was resected. Additionally, FA has been reported to be increased in the infiltrative peritumoral edema surrounding high-grade gliomas as compared to the vasogenic edema surrounding metastases.[89,90] Often, tumor boundaries are not clearly delineated by conventional imaging, and DTI tractography may improve border characterization leading to greater resection and improved outcomes.[87,91] The identification and preservation of white matter tracts is also important in preserving the neurological functional integrity of patients undergoing resection of lesions near eloquent cortex.

DTI-based tractography is fundamentally limited because a single tensor can only resolve a single fiber direction within

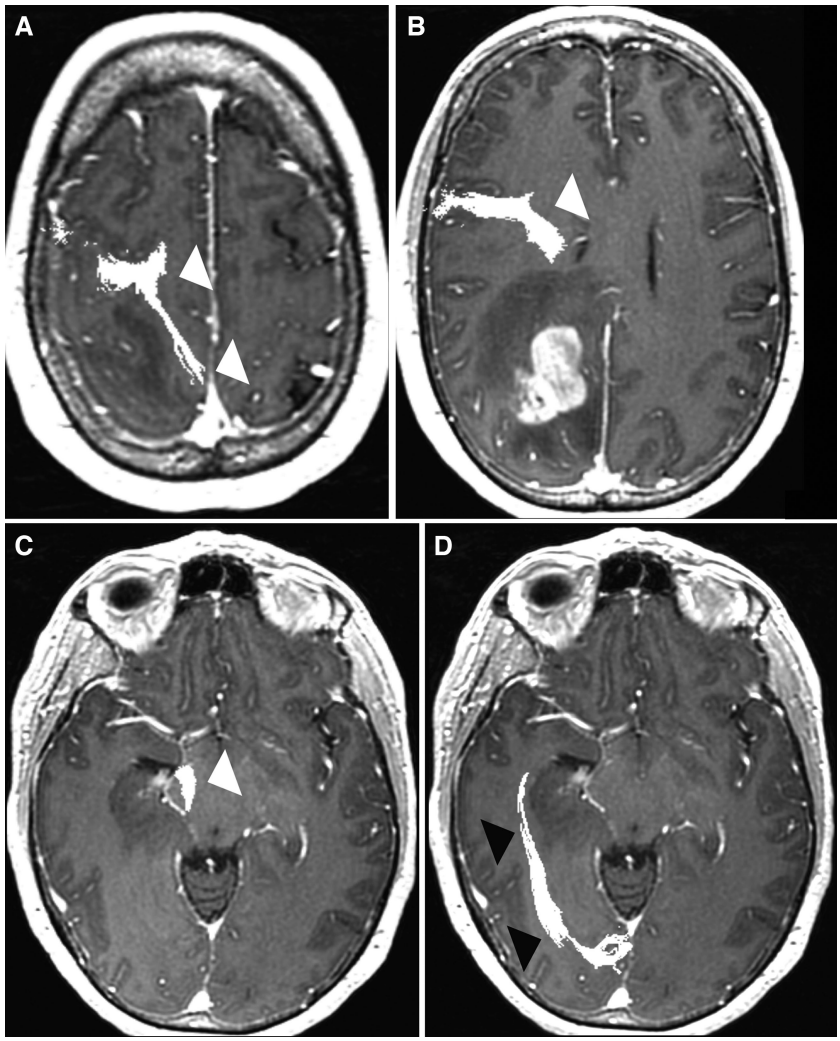

FIGURE 6. *DTI tractography in glioblastoma. A 58-yr-old woman with glioblastoma. Presurgical imaging included axial postcontrast T1 sequence with corticospinal tract DTI overlay* **A**-**C** *and optic radiation DTI overlay* **D**. *A large right parietotemporal mass splays the corticospinal tract superiorly (***A***; white arrowheads) and anteriorly displaces the descending tracts (***B***, ***C***; white arrowheads). The optic radiations are also displaced laterally by tumor (***D***; black arrowheads).*

an imaging voxel, while up to 90% of white matter voxels in the brain may contain multiple fibers.[92,93] As a result, many higher-order models are being investigated to address the so-called crossing fiber problem.[94] However, these developments have not yet translated into improvements in clinical practice.

Functional MRI

fMRI indirectly measures neuronal activity using the ratio of deoxyhemoglobin to oxyhemoglobin as a contrast mechanism, known as blood oxygen level dependent (BOLD) signal. fMRI can be used to for sensory motor, language, and memory mapping—all of which have important implications for presurgical planning and intraoperative navigation.[95-97]

In task-based fMRI, the patient alternates between a passive resting state and task performance, usually motor or language function, while relative changes in BOLD signal are measured and used to infer areas of cortical activation (Figure 8). Anatomic areas localized with task-based fMRI have been validated to approximate functional sites identified with cortical stimulation mapping. Apart from localizing eloquent cortex, task-based fMRI can be used to characterize tumors. Decreased BOLD signal is noted in cortex involved by tumor and differences are also seen between high- and low-grade tumor suggesting alterations in

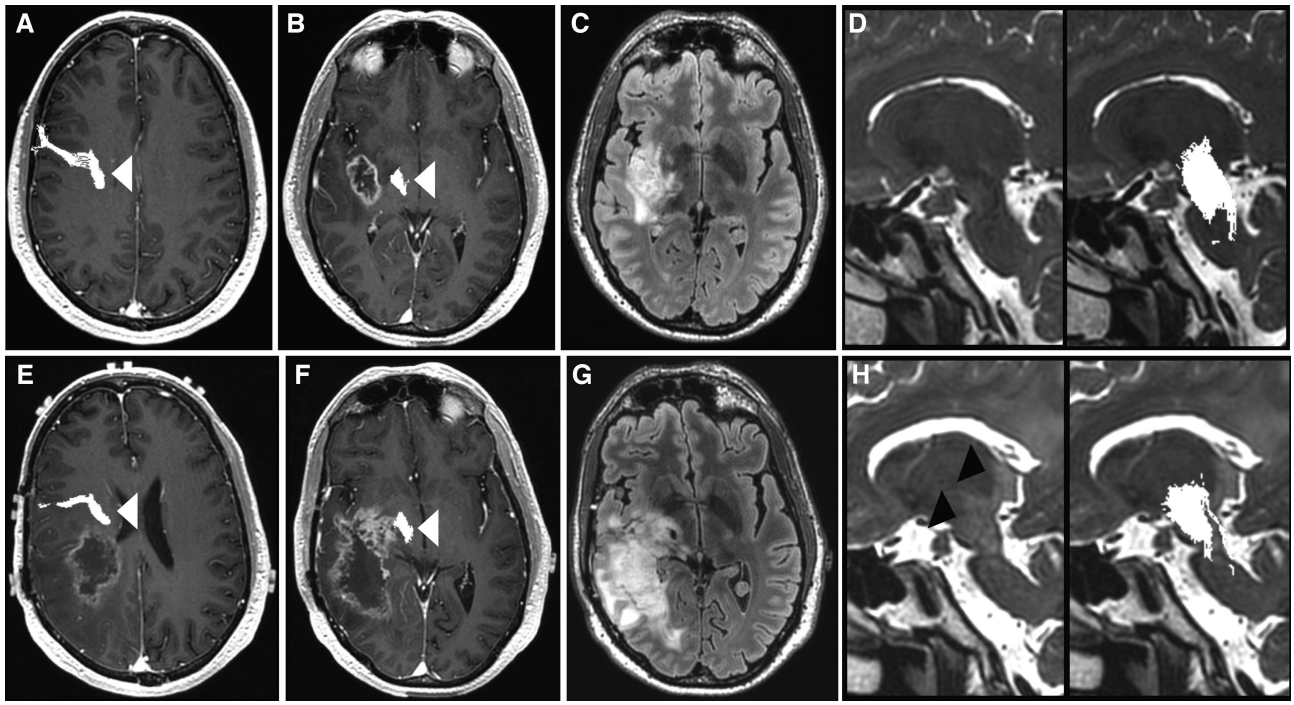

FIGURE 7. *DTI tractography in recurrent glioblastoma. A 48-yr-old man with glioblastoma before surgical resection (**A**-**D**) and 6 mo after completion of chemoradiotherapy **E**-**H**. Presurgical axial postcontrast T1 with right corticospinal tract DTI overlay **A**, **B** shows a peripherally enhancing right insular tumor separate from the corticospinal fibers (**A**, **B**; white arrowheads) and axial FLAIR shows adjacent infiltrative edema **C**. Sagittal T2 images without and with corticospinal tract DTI overlay show normal signal within the midbrain in the region of the descending corticospinal fibers **D**. Following chemoradiotherapy, axial postcontrast T1 with right corticospinal tract DTI overlay shows peripherally enhancing recurrent tumor inseparable from the descending corticospinal fibers (**E**, **F**; white arrowheads) and increased infiltrative edema along the descending tracts on axial FLAIR **G**. Sagittal T2 images without and with corticospinal tract DTI overlay now shows abnormal signal within the midbrain in the region of the descending corticospinal fibers (**H**; black arrowheads).*

cerebral blood volume of the tumor affected area.[98,99] fMRI can also be applied to guide DTI by delineating a seed region for fiber tractography.[100-102]

Recently, there has been increased interest in resting state functional MRI (rs-fMRI), which does not require patient cooperation with task paradigms and can be performed under anesthesia. rs-fMRI detects spontaneous low-frequency fluctuations in the BOLD signal between regions that are spatially distinct to identify functional networks, so-called resting state networks (RSNs).[103,104] The most fundamental RSN is the default mode network (DMN) and evidence regarding other RSNs including somatosensory, visual, auditory, language, attention, and cognitive control networks is evolving.[105] Compared with task-based fMRI, rs-fMRI has the ability to identify many networks simultaneously, thereby providing more comprehensive information on the functional architecture of the brain while reducing imaging time. Although the bulk of investigation has focused on functional connectivity and cognition, a few small studies have reported the use of rs-fMRI to depict changes in vascular physiology and tumor grade as well as predict postsurgical neurological changes.[106,107] While these studies are promising, further work is needed before rs-fMRI can be used routinely in the clinical setting.

IMAGING OF TREATMENT RESPONSE

Assessing brain tumor treatment response by MRI presents considerable challenges—not the least of which is determining tumor growth—and is fraught with pitfalls such as differentiating progression from treatment-related changes.

Current standard of care for glioblastoma involves maximal safe resection followed by concurrent chemoradiotherapy and adjuvant temozolomide.[108] Progressive disease is treated with antiangiogenic agents (eg, bevacizumab) and/or nitrosourea alkylating agents (eg, lomustine).[109,110] Gliomas of lower grades are treated with resection and some combination of chemoradiotherapy as adjuvant therapy or for recurrence.[111,112] Treatment of metastases primarily depends on their number, with solitary lesions amenable to resection whereas multiple lesions are often treated radiosurgically.[113-115] CNS lymphoma is treated with steroids and methotrexate with radiotherapy usually reserved for recurrent, chemotherapy-resistant, disease.[116,117] Moreover,

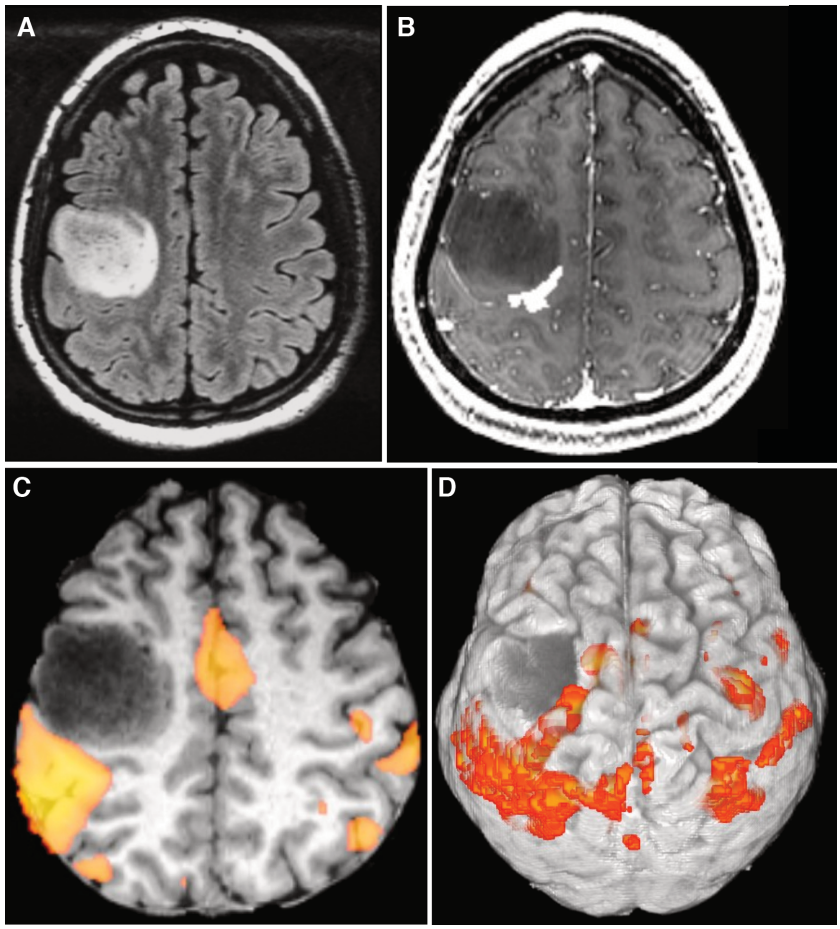

FIGURE 8. *Task-based fMRI in diffuse astrocytoma. A 22-yr-old man with diffuse astrocytoma. Axial FLAIR (**A**) and postcontrast T1 (**B**) MRI shows a nonenhancing right posterior frontal mass. DTI overlay of the corticospinal tract on postcontrast T1 images (**B**) shows medial displacement of the white matter fibers. Axial (**C**) and volume rendered (**D**) BOLD fMRI shows sensorimotor activation lateralized to the right peri-Rolandic cortex in response to left finger tapping with the anterior aspect of sensorimotor activation overlapping with the posterior margin of the mass. Left peri-Rolandic cortical activation is also seen in response to right finger tapping.*

numerous investigational therapies are available for a variety of indications. Any one of these therapies can either mimic or mask disease progression. And despite our state-of-the-art imaging techniques, serial imaging is often the most helpful and reliable noninvasive method to assess disease activity.

Brain tumor follow-up imaging reflects both treatment effect and natural evolution of tumor. Typically, increasing contrast enhancement and increasing nonenhancing signal abnormality represent progressive disease (Figure 9). Increasing contrast enhancement is particularly concerning for progression if it is seen at locations distant from the treatment site. However, it is important to keep in mind that small areas of reduced diffusion surrounding the resection cavity noted on immediate postoperative MRI, representing devitalized tumor or ischemic brain, often develop contrast enhancement at short term follow-up. Progressive nonenhancing disease can be suggested if the abnormality is of intermediate T2/FLAIR signal intensity, exerts mass effect upon adjacent structures, involves the cortex, or is associated with reduced diffusion or elevated perfusion. Furthermore, a spectrum of changes, not infrequently mimicking progression or response to therapy, are seen on MRI in the weeks to months to years following chemoradiation.[118,119]

Pseudoprogression

Pseudoprogression, an inflammatory response marked by a transient increase in contrast enhancement and edema upon

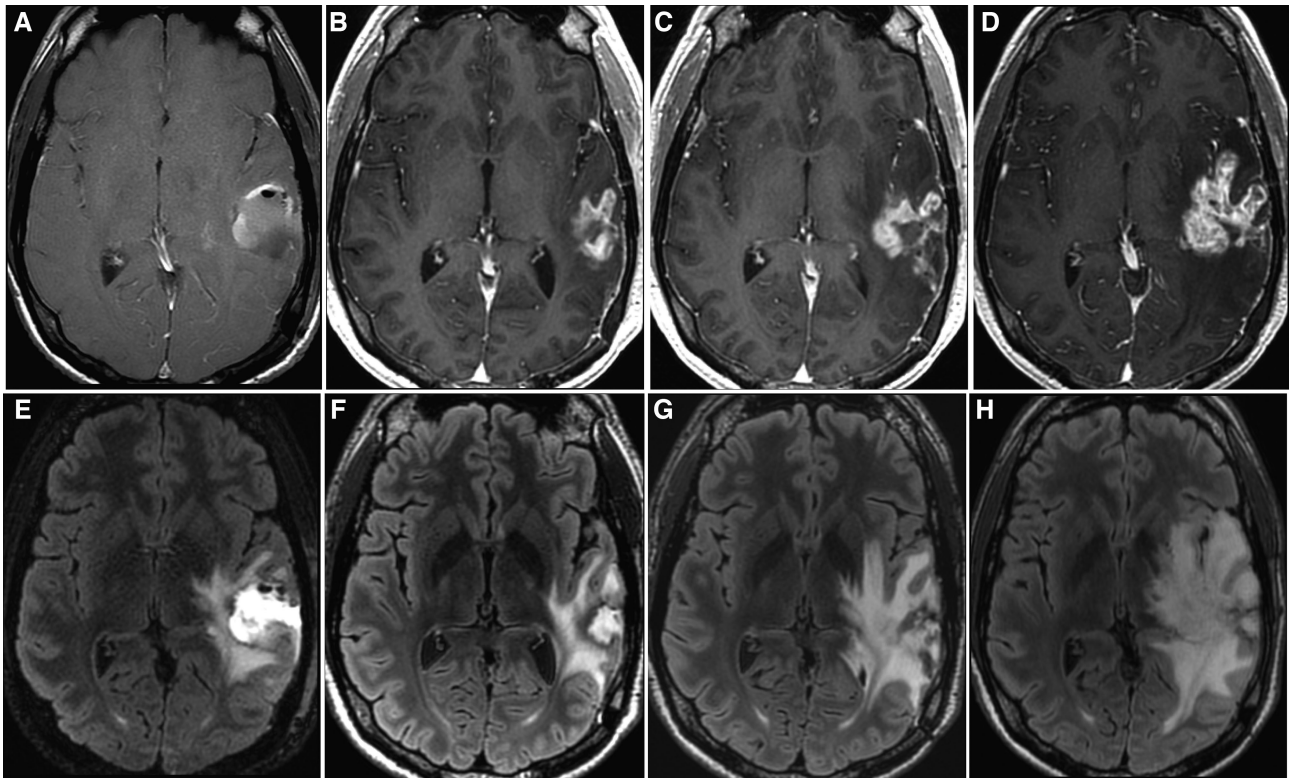

FIGURE 9. *Progressive disease. A 38-yr-old man with glioblastoma. Axial postcontrast T1 (**A**-**D**) and FLAIR (**E**-**H**) images demonstrate a left temporal resection cavity with minimal peripheral residual enhancement (**A**) and surrounding nonenhancing FLAIR signal abnormality **E**. At completion of chemoradiotherapy, increased enhancement is seen about the resection cavity, which is decreasing in size (**B**) and is associated with decreased surrounding FLAIR signal abnormality including decreased mass effect upon the left lateral ventricle **F**. MRI performed 2 mo later demonstrates increased enhancement (**C**) and increased ill-defined, mass-like, nonenhancing FLAIR signal abnormality **G**. Follow-up MRI performed 1 mo later shows continued increase in enhancing mass (**D**) and extent of expansile, ill-defined, nonenhancing FLAIR signal abnormality (**H**) consistent with progressive disease.*

completion of chemoradiotherapy, is observed in up to 30% of high-grade glioma patients and can also be seen in the setting of low-grade glioma. The hallmark of pseudoprogression is subsequent stabilization or improvement of contrast enhancement at follow-up MRI (Figure 10). Pseudoprogression occurs more frequently in tumors harboring O^6-methylguanine DNA methyltransferase (MGMT) promoter methylation and is associated with improved survival.[120-126] Pseudoprogression typically occurs within the first 3 mo following therapy and it is thought to represent a milder form of radiation necrosis, which manifests as a mass lesion with an appearance similar to recurrent tumor months to years postirradiation.[127,128] Since both pseudoprogression and true tumor progression share pathophysiology characterized by an underlying disruption of the BBB, it is difficult to differentiate the 2 processes using conventional imaging. In light of this difficulty, the updated Response Assessment in Neuro-Oncology (RANO) criteria stipulate that within the first 12 wk following completion of radiotherapy, progression can only be determined if new enhancement is seen outside of the radiation field or if there is histopathological confirmation of tumor growth.[14] Unfortunately, misdiagnoses can lead to under or overtreatment with potentially devastating clinical consequences.

Due to inherent risks of re-operation, major efforts have been made to better characterize increased contrast enhancement seen on postradiotherapy MRI. Although there are no definitive conventional MRI features with negative predictive value for pseudoprogression, some findings, such as multifocality, signal abnormality extending across the corpus callosum, and subependymal involvement, are suggestive of progression.[128,129] Higher ADC values have been observed in pseudoprogression, perhaps related to vasogenic edema of the inflammatory treatment effect, compared to lower ADC values in progressive, cellular disease.[130-132] While several studies have shown that decreased Cho and the presence of lipids and lactate are correlated with radiation necrosis, MRS of pseudoprogression remains variable.[133-138] Using DSC, DCE, and ASL techniques, lower

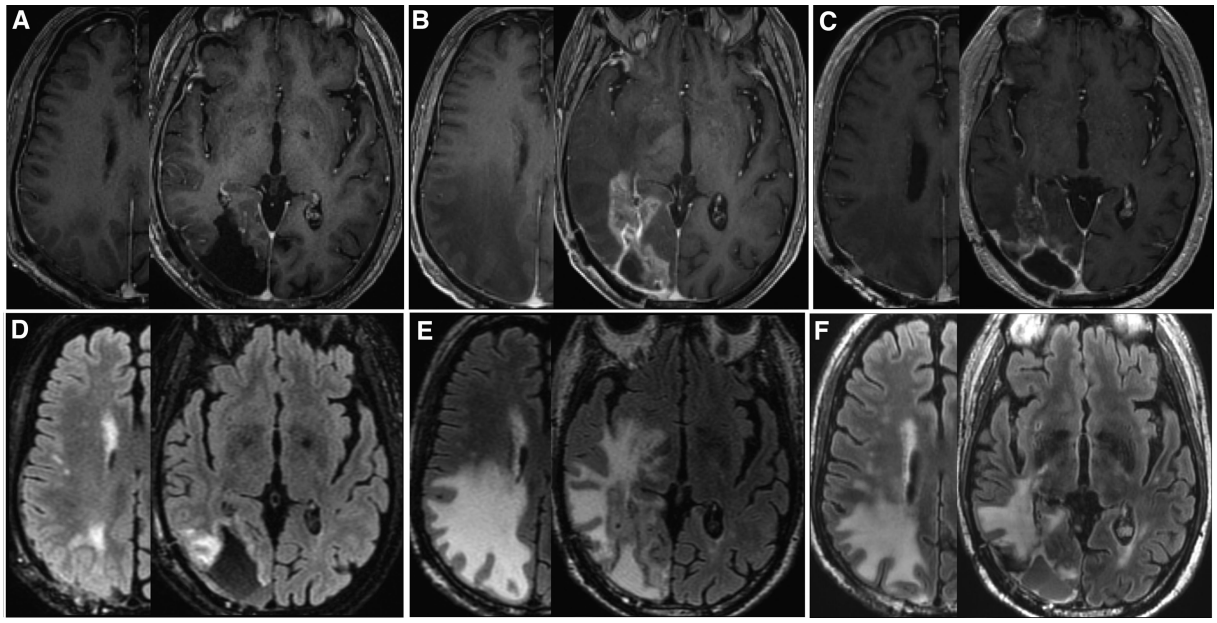

FIGURE 10. *Pseudoprogression. An 84-yr-old man with glioblastoma. Axial postcontrast T1 (**A**-**C**) and FLAIR (**D**-**F**) images at levels superior to and at a right parietal resection cavity demonstrate gross total resection of enhancing tumor (**A**) with minimal surrounding nonenhancing white matter signal abnormality **D**. At completion of chemoradiotherapy, new pericavity enhancement is seen (**B**) and extensive edema has developed **E**. Follow-up imaging 1 mo later without alteration of therapy demonstrates decreased enhancement (**C**) and edema (**F**) consistent with pseudoprogression.*

perfusion parameters have been shown in pseudoprogression compared to progressive disease with varying sensitivity and specificity.[135,139-142] Multiparametric models incorporating diffusivity, spectroscopy, and perfusion parameters among other imaging and clinical features have been used to better identify and predict progressive disease.[143-146] Despite these promising findings, prospective data and radiological–pathological correlation are lacking. Other advanced techniques currently being investigated include nuclear imaging agents, although their use in broad clinical practice is limited and beyond the scope of this review.[109,147,148]

Pseudoresponse

Pseudoresponse represents a marked decrease in contrast enhancement on MRI related to diminished leakiness of the BBB following treatment with antiangiogenic agents, most commonly bevacizumab, in patients with recurrent glioblastoma. The marked decrease in contrast enhancement, and often in peritumoral edema, can be observed as early as 1 day after initiation of antiangiogenic therapy and does not necessarily reflect biological antitumor effect of therapy (Figure 11).[119,149,150] Antiangiogenic agents may select for a hypoxic and invasive tumor phenotype that is capable of co-opting existing vasculature and therefore growing as nonenhancing infiltrative tumor before manifesting as progressive enhancing disease.[151,152] Progressive enhancement following antiangiogenic therapy has been shown to be a poor prognostic marker.[153] Low ADC values, representing viable cellular tumor, are seen in persistent or progressive nonenhancing tumor.[154,155] However, reduced diffusion may represent cytotoxic treatment effect and accurate interpretation requires serial imaging to assess temporal changes.[119,150,156] MRS has been investigated in the setting of antiangiogenic therapy; however, experience remains limited.[157-159] PWI has been used to characterize changes in tumor vasculature in response to therapy with decreased perfusion seen both in tumor and normal appearing brain.[159] Similar to changes in contrast enhancement, PWI can change rapidly and studies have shown that patients whose tumors showed normalized perfusion parameters after therapy had improved outcomes.[119] As with pseudoresponse, the use of multiparametic MRI shows promise in better characterizing regions of signal abnormality.[146,160]

Considering the importance of the nonenhancing tumor, the updated RANO criteria incorporate T2/FLAIR imaging characteristics as measures of response and define pseudoresponse as a greater than 50% reduction in contrast enhancement without a significant decrease in nonenhancing tumor. Decreased enhancement should persist for greater than 4 wk to be considered a true response.[14] While the RANO criteria do not account for all of the subtleties and nuances of evaluation of the post-treatment brain, they provide our current best framework to standardize response to treatment in gliomas.[161,162]

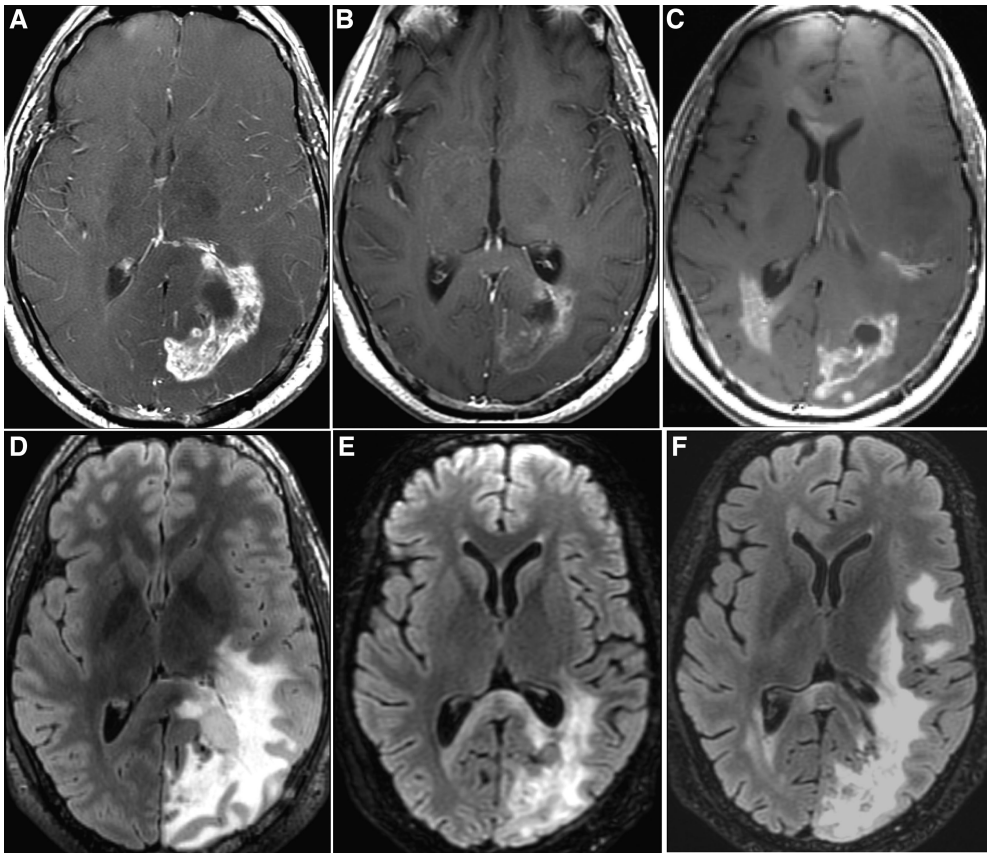

FIGURE 11. *Pseudoresponse. A 33-yr-old man with glioblastoma. Axial postcontrast T1 (**A**-**C**) and FLAIR (**D**-**F**) images demonstrate a left parietal mass with nodular enhancement and infiltrative edema prior to initiation of antiangiogenic therapy **A**, **D**. Four weeks after antiangiogenic therapy, a marked decrease in contrast enhancement and edema is seen **B**, **E**. Twelve weeks after antiangiogenic therapy, multifocal disease progression is seen in the right periatrial white matter, genu of the corpus callosum, and about the resection cavity **C**, **F**.*

Long-Term Complications of Therapy

In addition to mimics of tumor progression, several other chronic changes attributable to brain tumor therapy are well cataloged. Symmetric white matter signal abnormality representing gradual demyelination, gliosis, and vascular injury following chemotherapy, radiotherapy, or both is associated with progressive neurocognitive decline and disordered white matter diffusion.[163-166] In extreme cases, a diffuse necrotizing leukoencephalopathy can develop following intrathecal chemotherapy without or with radiotherapy.[167] Rarely, patients with a remote history of intracranial irradiation present with headaches and neurological deficits and are found to have abnormal cortical enhancement. This entity has been termed stroke-like migraine attacks after radiation therapy (SMART) syndrome and is self-limited with resolution of imaging findings and symptoms the course of weeks (Figure 12).[168] Additionally, with increased adoption of SWI in routine neuroimaging scattered foci of susceptibility are readily identified in the years following irradiation. While their pathogenesis is not fully understood, these small microhemorrhages or vascular malformations are thought to represent delayed radiation toxicity on cerebral microvasculature (Figure 13).[127,169,170]

Another late adverse effect of radiation therapy is the development of a second neoplasm. Radiation-associated tumors, in decreasing order of frequency, include meningioma, gliomas, and sarcomas.[171,172] The risk of developing a radiation-associated meningioma increases and latency to manifestation decreases with increasing radiation dose. Radiation-associated meningiomas tend to occur at a younger age and are more often multiple when contrasted with sporadic meningiomas (Figure 13).[173,174] Radiation-associated gliomas are usually a high-grade astrocytoma occurring in the radiation field with imaging features indistinguishable from a primary glioma.[171]

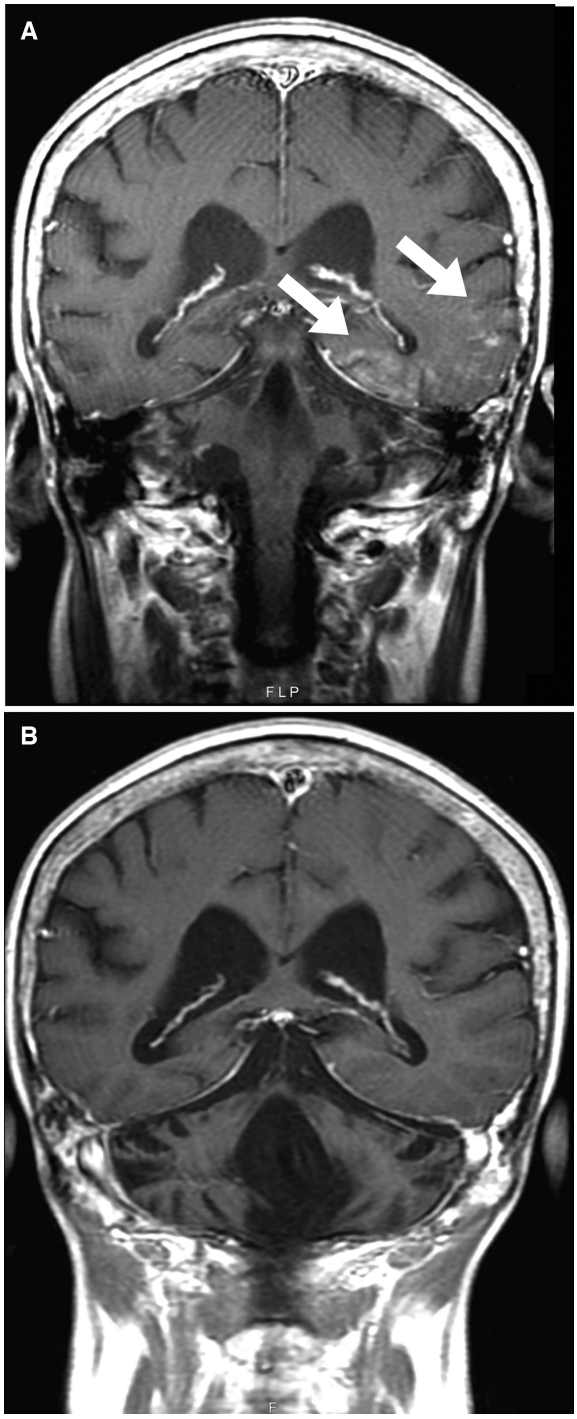

FIGURE 12. *SMART syndrome. A 44-yr-old woman with previously resected oligodendroglioma treated with adjuvant radiotherapy presented with headaches and aphasia. Coronal postcontrast T1 MRI at presentation demonstrates left temporal gyral enhancement (A; white arrows). Follow-up MRI at 4 wk with resolution of symptoms demonstrates resolution of left temporal gyral enhancement B.*

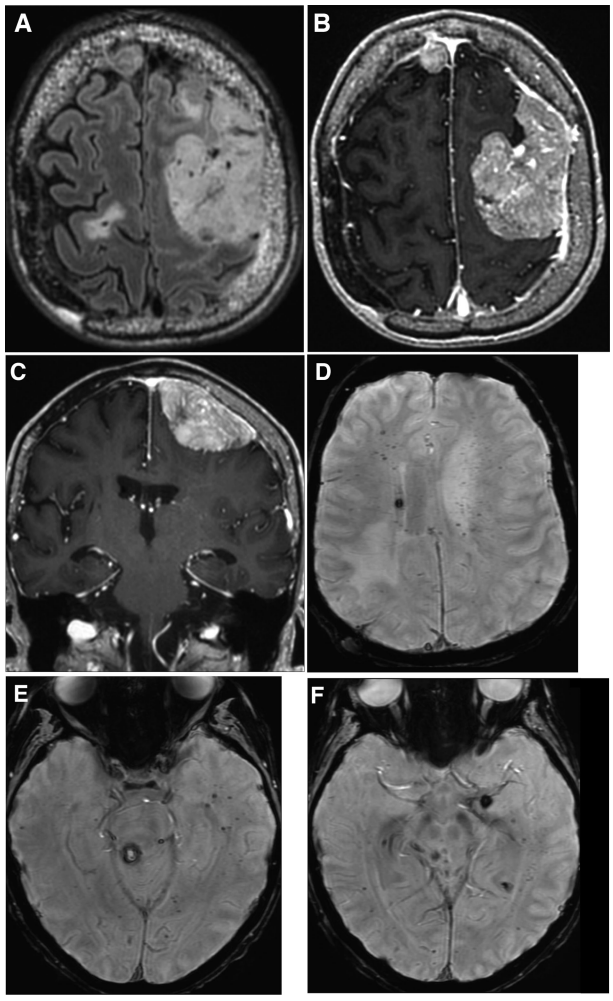

FIGURE 13. *Radiation-associated neoplasm and microhemorrhage. A 52-yr-old man with history of unknown brain tumor treated with irradiation 30 yr prior to presentation. Axial FLAIR (A) and axial (B) and coronal (C) postcontrast T1 MR images demonstrate enhancing extra-axial masses in the right and left frontal convexities with mild underlying parenchymal edema compatible with radiation-associated meningiomas. Axial SWI (D-F) images demonstrate multiple scattered foci of susceptibility compatible with postradiation microvascular injury.*

CONCLUSION

The past several decades have seen the widespread adoption of advanced MRI techniques in addition to conventional structural MRI for the routine clinical assessment of brain tumors. The incorporation of these biology-driven MRI methods has been indispensable to the neurosurgeon and contributed to improved diagnosis, surgical and radiosurgical planning, and assessment of treatment response. Neuroimaging will continue to evolve to reflect our growing understanding of brain tumor molecular genetics and targeted therapy with the overarching goal of being

the objective and quantitative arbiter of therapy response for patients with brain tumor.

Disclosures

JEV was supported by an NIH T32 grant (5 T32 EB001631-12). The authors have no personal, financial, or institutional interest in any of the drugs, materials, or devices described in this article.

REFERENCES

1. Ellingson BM, Bendszus M, Boxerman J, et al. Consensus recommendations for a standardized Brain Tumor Imaging Protocol in clinical trials. *Neuro Oncol*. 2015;17(9):1188-1198.
2. Gumprecht HK, Widenka DC, Lumenta CB. BrainLab VectorVision Neuronavigation System: technology and clinical experiences in 131 cases. *Neurosurgery*. 1999;44(1):97-104.
3. Willems PWA, van der Sprenkel JWB, Tulleken CAF, Viergever MA, Taphoorn MJB. Neuronavigation and surgery of intracerebral tumours. *J Neurol*. 2006;253(9):1123-1136.
4. Elhawary H, Liu H, Patel P, et al. Intraoperative real-time querying of white matter tracts during frameless stereotactic neuronavigation. *Neurosurgery*. 2011;68(2):506-516; discussion 516.
5. Saconn PA, Shaw EG, Chan MD, et al. Use of 3.0-T MRI for stereotactic radiosurgery planning for treatment of brain metastases: a single-institution retrospective review. *Int J Radiat Oncol Biol Phys*. 2010;78(4):1142-1146.
6. Zhang B, MacFadden D, Damyanovich AZ, et al. Development of a geometrically accurate imaging protocol at 3 Tesla MRI for stereotactic radiosurgery treatment planning. *Phys Med Biol*. 2010;55(22):6601-6615.
7. Cha S. Update on brain tumor imaging. *Curr Neurol Neurosci Rep*. 2005;5(3):169-177.
8. Neuwelt EA. Mechanisms of disease: the blood-brain barrier. *Neurosurgery*. 2004;54(1):131-142.
9. Smirniotopoulos JG, Murphy FM, Rushing EJ, Rees JH, Schroeder JW. Patterns of contrast enhancement in the brain and meninges. *Radiographics*. 2007;27(2):525-551.
10. Stummer W. Mechanisms of tumor-related brain edema. *Neurosurg Focus*. 2007;22(5):1-7.
11. Nag S, Manias JL, Stewart DJ. Pathology and new players in the pathogenesis of brain edema. *Acta Neuropathol*. 2009;118(2):197-217.
12. Ginsberg LE, Fuller GN, Hashmi M, Leeds NE, Schomer DF. The significance of lack of MR contrast enhancement of supratentorial brain tumors in adults: histopathological evaluation of a series. *Surg Neurol*. 1998;49(4):436-440.
13. Barajas RF, Hess CP, Phillips JJ, et al. Super-resolution track density imaging of glioblastoma: histopathologic correlation. *AJNR Am J Neuroradiol*. 2013;34(7):1319-1325.
14. Wen PY, Macdonald DR, Reardon DA, et al. Updated response assessment criteria for high-grade gliomas: response assessment in Neuro-Oncology Working Group. *J Clin Oncol*. 2010;28(11):1963-1972.
15. Drevelegas A. Extra-axial brain tumors. *Eur Radiol*. 2005;15(3):453-467.
16. Cha S, Pierce S, Knopp EA, et al. Dynamic contrast-enhanced T2*-weighted MR imaging of tumefactive demyelinating lesions. *Am J Neuroradiol*. 2001;22(6):1109-1116.
17. Raz E, Zagzag D, Saba L, et al. Cyst with a mural nodule tumor of the brain. *Cancer Imaging*. 2012;12(1):237-244.
18. Tsuchiya K, Makita K, Furui S, Nitta K. MRI appearances of calcified regions within intracranial tumours. *Neuroradiology*. 1993;35(5):341-344.
19. Kondziolka D, Bernstein M, Resch L, et al. Significance of hemorrhage into brain tumors: clinicopathological study. *J Neurosurg*. 1987;67(6):852-857.
20. Yuguang L, Meng L, Shugan Z, Yuquan J, Gang L, Xingang L. Intracranial tumoural haemorrhage—a report of 58 cases. *J Clin Neurosci*. 2002;9(6):637-639.
21. Rubenstein J, Fischbein N, Aldape K, Burton E, Shuman M. Hemorrhage and VEGF expression in a case of primary CNS lymphoma. *J Neurooncol*. 2002;58(1):53-56.
22. Louis DN, Ohgaki H, Wiestler OD, et al. The 2007 WHO classification of tumours of the central nervous system. *Acta Neuropathol*. 2007;114(2):97-109.
23. Krishnatry R, Zhukova N, Guerreiro Stucklin AS, et al. Clinical and treatment factors determining long-term outcomes for adult survivors of childhood low-grade glioma: a population-based study. *Cancer*. 2016;122(8):1261-1269.
24. Nageswara Rao AA, Packer RJ. Advances in the management of low-grade gliomas. *Curr Oncol Rep*. 2014;16(8):1-8.
25. Cancer Genome Atlas Research Network. Comprehensive genomic characterization defines human glioblastoma genes and core pathways. *Nature*. 2008;455(7216):1061-1068.
26. Ohgaki H, Kleihues P. Genetic alterations and signaling pathways in the evolution of gliomas. *Cancer Sci*. 2009;100(12):2235-2241.
27. Horbinski C, Miller CR, Perry A. Gone FISHing: clinical lessons learned in brain tumor molecular diagnostics over the last decade. *Brain Pathol*. 2011;21(1):57-73.
28. Gupta K, Salunke P. Molecular markers of glioma: an update on recent progress and perspectives. *J Cancer Res Clin Oncol*. 2012;138(12):1971-1981.
29. Weller M, Pfister SM, Wick W, Hegi ME, Reifenberger G, Stupp R. Molecular neuro-oncology in clinical practice: a new horizon. *Lancet Oncol*. 2013;14(9):e370-e379.
30. Cancer Genome Atlas Research Network, Brat DJ, Verhaak RGW, et al. Comprehensive, integrative genomic analysis of diffuse lower-grade gliomas. *N Engl J Med*. 2015;372(26):2481-2498.
31. Eckel-Passow JE, Lachance DH, Molinaro AM, et al. Glioma groups based on 1p/19q, IDH, and TERT promoter mutations in tumors. *N Engl J Med*. 2015;372(26):2499-2508.
32. Louis DN, Perry A, Reifenberger G, et al. The 2016 World Health Organization Classification of Tumors of the Central Nervous System: a summary. *Acta Neuropathol*. 2016;131(6):803-820.
33. Mabray MC, Barajas RF Jr, Cha S. Modern brain tumor imaging. *Brain Tumor Res Treat*. 2015;3(1):8-16.
34. Moseley ME, Butts K, Yenari MA, Marks M, Crespigny AD. Clinical aspects of DWI. *NMR Biomed*. 1995;8(7):387-396.
35. Schaefer PW, Grant PE, Gonzalez RG. Diffusion-weighted MR imaging of the brain. *Radiology*. 2000;217(2):331-345.
36. Bammer R, Holdsworth SJ, Veldhuis WB, Skare ST. New methods in diffusion-weighted and diffusion tensor imaging. *Magn Reson Imaging Clin N Am*. 2009;17(2):175-204.
37. Ebisu T, Tanaka C, Umeda M, et al. Discrimination of brain abscess from necrotic or cystic tumors by diffusion-weighted echo planar imaging. *Magn Reson Imaging*. 1996;14(9):1113-1116.
38. Chang SC, Lai PH, Chen WL, et al. Diffusion-weighted MRI features of brain abscess and cystic or necrotic brain tumors: comparison with conventional MRI. *Clin Imaging*. 2002;26(4):227-236.
39. Given CA, Stevens BS, Lee C. The MRI appearance of tumefactive demyelinating lesions. *Am J Roentgenol*. 2004;182(1):195-199.
40. Yamasaki F, Kurisu K, Satoh K, et al. Apparent diffusion coefficient of human brain tumors at MR imaging. *Radiology*. 2005;235(3):985-991.
41. Herneth AM, Guccione S, Bednarski M. Apparent diffusion coefficient: a quantitative parameter for in vivo tumor characterization. *Eur J Radiol*. 2003;45(3):208-213.
42. Al-Okaili RN, Krejza J, Wang S, Woo JH, Melhem ER. Advanced MR imaging techniques in the diagnosis of intraaxial brain tumors in adults. *Radiographics*. 2006;26 (suppl 1):S173-S189.
43. Tozer DJ, Jäger HR, Danchaivijitr N, et al. Apparent diffusion coefficient histograms may predict low-grade glioma subtype. *NMR Biomed*. 2007;20(1):49-57.
44. Xiao H-F, Chen Z-Y, Lou X, et al. Astrocytic tumour grading: a comparative study of three-dimensional pseudocontinuous arterial spin labelling, dynamic susceptibility contrast-enhanced perfusion-weighted imaging, and diffusion-weighted imaging. *Eur Radiol*. 2015;25(12):3423-3430.
45. Barajas RF, Rubenstein JL, Chang JS, Hwang J, Cha S. Diffusion-weighted MR imaging derived apparent diffusion coefficient is predictive of clinical outcome in primary central nervous system lymphoma. *Am J Neuroradiol*. 2009;31(1):60-66.
46. Pauleit D, Langen K-J, Floeth F, et al. Can the apparent diffusion coefficient be used as a noninvasive parameter to distinguish tumor tissue from peritumoral tissue in cerebral gliomas? *J Magn Reson Imaging*. 2004;20(5):758-764.
47. Chiang IC, Kuo Y-T, Lu C-Y, et al. Distinction between high-grade gliomas and solitary metastases using peritumoral 3-T magnetic resonance spectroscopy, diffusion, and perfusion imagings. *Neuroradiology*. 2004;46(8). doi:10.1007/s00234-004-1246-7.

48. Stadnik TW, Chaskis C, Michotte A, et al. Diffusion-weighted MR imaging of intracerebral masses: comparison with conventional MR imaging and histologic findings. *Am J Neuroradiol*. 2001;22(5):969-976.
49. Pierce T, Kranz P, Roth C, Leong D, Wei P, Provenzale JM. Use of apparent diffusion coefficient values for diagnosis of pediatric posterior fossa tumors. *Neuroradiol J*. 2014;27(2). doi:10.15274/NRJ-2014-10027.
50. Ellingson BM, Sahebjam S, Kim HJ, et al. Pretreatment ADC histogram analysis is a predictive imaging biomarker for bevacizumab treatment but not chemotherapy in recurrent glioblastoma. *Am J Neuroradiol*. 2014;35(4):673-679.
51. Kang Y, Choi SH, Kim Y-J, et al. Gliomas: Histogram analysis of apparent diffusion coefficient maps with standard- or high-b-value diffusion-weighted MR imaging–correlation with tumor grade. *Radiology*. 2011;261(3):882-890.
52. Haacke EM, Mittal S, Wu Z, Neelavalli J, Cheng YCN. Susceptibility-weighted imaging: technical aspects and clinical applications, part 1. *AJNR Am J Neuroradiol*. 2009;30(1):19-30.
53. Mittal S, Wu Z, Neelavalli J, Haacke EM. Susceptibility-weighted imaging: technical aspects and clinical applications, part 2. *AJNR Am J Neuroradiol*. 2009;30(2):232-252.
54. Radbruch A, Wiestler B, Kramp L, et al. Differentiation of glioblastoma and primary CNS lymphomas using susceptibility weighted imaging. *Eur J Radiol*. 2013;82(3):552-556.
55. Brodbelt A. Clinical applications of imaging biomarkers. Part 2. The neurosurgeon's perspective. *Br J Radiol*. 2011;84(special_issue_2):S205-S208.
56. Barajas RF, Hodgson JG, Chang JS, et al. Glioblastoma multiforme regional genetic and cellular expression patterns: influence on anatomic and physiologic MR imaging. *Radiology*. 2010;254(2):564-576.
57. Essig M, Nguyen TB, Shiroishi MS, et al. Perfusion MRI: the five most frequently asked clinical questions. *Am J Roentgenol*. 2013;201(3):W495-W510.
58. Cha S, Tihan T, Crawford F, et al. Differentiation of low-grade oligodendrogliomas from low-grade astrocytomas by using quantitative blood-volume measurements derived from dynamic susceptibility contrast-enhanced MR imaging. *Am J Neuroradiol*. 2005;26(2):266-273.
59. Cha S, Lupo JM, Chen MH, et al. Differentiation of glioblastoma multiforme and single brain metastasis by peak height and percentage of signal intensity recovery derived from dynamic susceptibility-weighted contrast-enhanced perfusion MR imaging. *Am J Neuroradiol*. 2007;28(6):1078-1084.
60. Law M, Young RJ, Babb JS, et al. Gliomas: predicting time to progression or survival with cerebral blood volume measurements at dynamic susceptibility-weighted contrast-enhanced perfusion MR imaging 1. *Radiology*. 2008;247(2):490-498.
61. Griffith B, Jain R. Perfusion imaging in neuro-oncology. *Radiol Clin North Am*. 2015;53(3):497-511.
62. Jain R. Measurements of tumor vascular leakiness using DCE in brain tumors: clinical applications. *NMR Biomed*. 2013;26(8):1042-1049.
63. Roberts HC, Roberts TP, Brasch RC, Dillon WP. Quantitative measurement of microvascular permeability in human brain tumors achieved using dynamic contrast-enhanced MR imaging: correlation with histologic grade. *Am J Neuroradiol*. 2000;21(5):891-899.
64. Roberts HC, Roberts TPL, Ley S, Dillon WP, Brasch RC. Quantitative estimation of microvascular permeability in human brain tumors. *Acad Radiol*. 2002;9(1):S151-S155.
65. Patankar TF, Haroon HA, Mills SJ, et al. Is volume transfer coefficient (K(trans)) related to histologic grade in human gliomas? *Am J Neuroradiol*. 2005;26(10):2455-2465.
66. Watts JM, Whitlow CT, Maldjian JA. Clinical applications of arterial spin labeling. *NMR Biomed*. 2013;26(8):892-900.
67. White CM, Pope WB, Zaw T, et al. Regional and voxel-wise comparisons of blood flow measurements between dynamic susceptibility contrast magnetic resonance imaging (DSC-MRI) and arterial spin labeling (ASL) in brain tumors. *J Neuroimag*. 2012;24(1):23-30.
68. Kim MJ, Kim HS, Kim JH, Cho KG, Kim SY. Diagnostic accuracy and interobserver variability of pulsed arterial spin labeling for glioma grading. *Acta Radiol*. 2008;49(4):450-457.
69. Fudaba H, Shimomura T, Abe T, et al. Comparison of multiple parameters obtained on 3T pulsed arterial spin-labeling, diffusion tensor imaging, and MRS and the Ki-67 labeling index in evaluating glioma grading. *Am J Neuroradiol*. 2014;35(11):2091-2098.
70. Cebeci H, Aydin O, Ozturk-Isik E, et al. Assesment of perfusion in glial tumors with arterial spin labeling; comparison with dynamic susceptibility contrast method. *Eur J Radiol*. 2014;83(10):1914-1919.
71. Furtner J, Bender B, Braun C, et al. Prognostic value of blood flow measurements using arterial spin labeling in gliomas. *PLoS One*. 2014;9(6):e99616. doi:10.1371/journal.pone.0099616.
72. Qiao XJ, Ellingson BM, Kim HJ, et al. Arterial spin-labeling perfusion MRI stratifies progression-free survival and correlates with epidermal growth factor receptor status in glioblastoma. *Am J Neuroradiol*. 2015;36(4):672-677.
73. Soares DP, Law M. Magnetic resonance spectroscopy of the brain: review of metabolites and clinical applications. *Clin Radiol*. 2009;64(1):12-21.
74. Horská A, Barker PB. Imaging of brain tumors: MR spectroscopy and metabolic imaging. *Neuroimaging Clin North Am*. 2010;20(3):293-310.
75. Lin A, Tran T, Bluml S, Merugumala S, Liao H-J, Ross BD. Guidelines for acquiring and reporting clinical neurospectroscopy. *Semin Neurol*. 2012;32(4):432-453.
76. Bulik M, Jancalek R, Vanicek J, Skoch A, Mechl M. Potential of MR spectroscopy for assessment of glioma grading. *Clin Neurol Neurosurg*. 2013;115(2):146-153.
77. McKnight TR, Bussche von dem MH, Vigneron DB, et al. Histopathological validation of a three-dimensional magnetic resonance spectroscopy index as a predictor of tumor presence. *J Neurosurg*. 2002;97(4):794-802.
78. Fountas KN, Kapsalaki EZ, Vogel RL, Fezoulidis I, Robinson JS, Gotsis ED. Noninvasive histologic grading of solid astrocytomas using proton magnetic resonance spectroscopy. *Stereotact Funct Neurosurg*. 2004;82(2-3):90-97.
79. Huang Y, Lisboa PJG, El-Deredy W. Tumour grading from magnetic resonance spectroscopy: a comparison of feature extraction with variable selection. *Stat Med*. 2002;22(1):147-164.
80. Hourani R, Brant LJ, Rizk T, Weingart JD, Barker PB, Horska A. Can proton MR spectroscopic and perfusion imaging differentiate between neoplastic and nonneoplastic brain lesions in adults? *Am J Neuroradiol*. 2008;29(2):366-372.
81. Castillo M, Smith JK, Kwock L. Correlation of myo-inositol levels and grading of cerebral astrocytomas. *Am J Neuroradiol*. 2000;21(9):1645-1649.
82. Server A, Josefsen R, Kulle B, et al. Proton magnetic resonance spectroscopy in the distinction of high-grade cerebral gliomas from single metastatic brain tumors. *Acta Radiol*. 2010;51(3):316-325.
83. Narayana A, Chang J, Thakur S, et al. Use of MR spectroscopy and functional imaging in the treatment planning of gliomas. *Br J Radiol*. 2007;80(953):347-354.
84. Law M, Cha S, Knopp EA, Johnson G, Arnett J, Litt AW. High-grade gliomas and solitary metastases: differentiation by using perfusion and proton spectroscopic MR imaging. *Radiology*. 2002;222(3):715-721.
85. Ken S, Vieillevigne L, Franceries X, et al. Integration method of 3D MR spectroscopy into treatment planning system for glioblastoma IMRT dose painting with integrated simultaneous boost. *Radiat Oncol*. 2013;8(1):1. doi:10.1186/1748-717X-8-1.
86. Zhang J, Zhuang D-X, Yao C-J, et al. Metabolic approach for tumor delineation in glioma surgery: 3D MR spectroscopy image-guided resection. *J Neurosurg*. 2016;124(6):1585-1593.
87. Shahar T, Rozovski U, Marko NF, et al. Preoperative imaging to predict intraoperative changes in tumor-to-corticospinal tract distance. *Neurosurgery*. 2014;75(1):23-30.
88. Coenen VA, Krings T, Mayfrank L, et al. Three-dimensional visualization of the pyramidal tract in a neuronavigation system during brain tumor surgery: first experiences and technical note. *Neurosurgery*. 2001;49(1):86-93.
89. Byrnes TJD, Barrick TR, Bell BA, Clark CA. Diffusion tensor imaging discriminates between glioblastoma and cerebral metastases in vivo. *NMR Biomed*. 2011;24(1):54-60.
90. Lu S, Ahn D, Johnson G, Law M, Zagzag D, Grossman RI. Diffusion-tensor MR imaging of intracranial neoplasia and associated peritumoral edema: introduction of the tumor infiltration index. *Radiology*. 2004;232(1):221-228.
91. Yan J-L, van der Hoorn A, Larkin TJ, Boonzaier NR, Matys T, Price SJ. Extent of resection of peritumoral diffusion tensor imaging–detected abnormality as a predictor of survival in adult glioblastoma patients. *J Neurosurg*. 2017;126(1):234-241.

92. Farquharson S, Tournier JD, Calamante F, et al. White matter fiber tractography: why we need to move beyond DTI. *J Neurosurg*. 2013;118(6):1367-1377.
93. Mandelli ML, Berger MS, Bucci M, Berman JI, Amirbekian B, Henry RG. Quantifying accuracy and precision of diffusion MR tractography of the corticospinal tract in brain tumors. *J Neurosurg*. 2014;121(2):349-358.
94. Potgieser ARE, Wagemakers M, van Hulzen ALJ, de Jong BM, Hoving EW, Groen RJM. The role of diffusion tensor imaging in brain tumor surgery: a review of the literature. *Clin Neurol Neurosurg*. 2014;124:51-58.
95. Nadkarni TN, Andreoli MJ, Nair VA, et al. Usage of fMRI for pre-surgical planning in brain tumor and vascular lesion patients: task and statistical threshold effects on language lateralization. *NeuroImage Clin*. 2015;7:415-423.
96. Bauer PR, Reitsma JB, Houweling BM, Ferrier CH, Ramsey NF. Can fMRI safely replace the Wada test for preoperative assessment of language lateralisation? A meta-analysis and systematic review. *J Neurol Neurosurg Psychiatry*. 2014;85(5):581-588.
97. Giussani C, Roux F-E, Ojemann J, Sganzerla EP, Pirillo D, Papagno C. Is preoperative functional magnetic resonance imaging reliable for language areas mapping in brain tumor surgery? Review of language functional magnetic resonance imaging and direct cortical stimulation correlation studies. *Neurosurgery*. 2010;66(1):113-120.
98. Wang L, Chen D, Olson J, Ali S, Fan T, Mao H. Re-examine tumor-induced alterations in hemodynamic responses of BOLD fMRI: implications in presurgical brain mapping. *Acta Radiol*. 2012;53(7):802-811.
99. Hou BL, Bradbury M, Peck KK, Petrovich NM, Gutin PH, Holodny AI. Effect of brain tumor neovasculature defined by rCBV on BOLD fMRI activation volume in the primary motor cortex. *NeuroImage*. 2006;32(2):489-497.
100. Kumar A, Chandra PS, Sharma BS, et al. The role of neuronavigation-guided functional MRI and diffusion tensor tractography along with cortical stimulation in patients with eloquent cortex lesions. *Br J Neurosurg*. 2014;28(2):226-233.
101. Schonberg T, Pianka P, Hendler T, Pasternak O, Assaf Y. Characterization of displaced white matter by brain tumors using combined DTI and fMRI. *NeuroImage*. 2006;30(4):1100-1111.
102. Kleiser R, Staempfli P, Valavanis A, Boesiger P, Kollias S. Impact of fMRI-guided advanced DTI fiber tracking techniques on their clinical applications in patients with brain tumors. *Neuroradiology*. 2009;52(1):37-46.
103. Leuthardt EC, Allen M, Kamran M, et al. Resting-state blood oxygen level-dependent functional MRI: a paradigm shift in preoperative brain mapping. *Stereotact Funct Neurosurg*. 2016;93(6):427-439.
104. Zhang D, Johnston JM, Fox MD, et al. Preoperative sensorimotor mapping in brain tumor patients using spontaneous fluctuations in neuronal activity imaged with functional magnetic resonance imaging: initial experience. *Neurosurgery*. 2009;65(6 suppl):226-236.
105. Lee MH, Smyser CD, Shimony JS. Resting-state fMRI: a review of methods and clinical applications. *Am J Neuroradiol*. 2013;34(10):1866-1872.
106. Roder C, Charyasz-Leks E, Breitkopf M, et al. Resting-state functional MRI in an intraoperative MRI setting: proof of feasibility and correlation to clinical outcome of patients. *J Neurosurg*. 2016;125(2):401-409.
107. Kuhnt D, Bauer MHA, Becker A, et al. Intraoperative visualization of fiber tracking based reconstruction of language pathways in glioma surgery. *Neurosurgery*. 2012;70(4):911-920.
108. Stupp R, Brada M, van den Bent MJ, Tonn JC, Pentheroudakis G, ESMO Guidelines Working Group . High-grade glioma: ESMO Clinical Practice Guidelines for diagnosis, treatment and follow-up. *Ann Oncol*. 2014;25 (suppl 3):iii93-iii101.
109. Neubeck von C, Seidlitz A, Kitzler HH, Beuthien-Baumann B, Krause M. Glioblastoma multiforme: emerging treatments and stratification markers beyond new drugs. *Br J Radiol*. 2015;88(1053):20150354. doi:10.1259/bjr.20150354.
110. Johnson DR, Leeper HE, Uhm JH. Glioblastoma survival in the United States improved after Food and Drug Administration approval of bevacizumab: a population-based analysis. *Cancer*. 2013;119(19):3489-3495.
111. Le Rhun E, Taillibert S, Chamberlain MC. Current management of adult diffuse infiltrative low grade gliomas. *Curr Neurol Neurosci Rep*. 2016;16(2). doi:10.1007/s11910-015-0615-4.
112. Duffau H, Taillandier L. New concepts in the management of diffuse low-grade glioma: proposal of a multistage and individualized therapeutic approach. *Neuro Oncol*. 2015;17(3):332-342.
113. Lippitz B, Lindquist C, Paddick I, Peterson D, O'Neill K, Beaney R. Stereotactic radiosurgery in the treatment of brain metastases: the current evidence. *Cancer Treat Rev*. 2014;40(1):48-59.
114. Tsao MN, Rades D, Wirth A, et al. Radiotherapeutic and surgical management for newly diagnosed brain metastasis(es): an American society for radiation oncology evidence-based guideline. *Pract Radiat Oncol*. 2012;2(3):210-225.
115. Hatiboglu MA, Wildrick DM, Sawaya R. The role of surgical resection in patients with brain metastases. *Ecancermedicalscience*. 2013;7:308. doi:10.3332/ecancer.2013.308.
116. Korfel A, Schlegel U. Diagnosis and treatment of primary CNS lymphoma. *Nat Rev Neurol*. 2013;9(6):317-327.
117. Schiff D, Lee EQ, Nayak L, Norden AD, Reardon DA, Wen PY. Medical management of brain tumors and the sequelae of treatment. *Neuro Oncol*. 2014;17(4):488-504.
118. Hygino da Cruz LC, Rodriguez I, Domingues RC, Gasparetto EL, Sorensen AG. Pseudoprogression and pseudoresponse: imaging challenges in the assessment of posttreatment glioma. *AJNR Am J Neuroradiol*. 2011;32(11):1978-1985.
119. Huang RY, Neagu MR, Reardon DA, Wen PY. Pitfalls in the neuroimaging of glioblastoma in the era of antiangiogenic and immuno/targeted therapy – detecting illusive disease, defining response. 2015;6(33):1-16.
120. de Wit MCY, de Bruin HG, Eijkenboom W, Sillevis Smitt PAE, van den Bent MJ. Immediate post-radiotherapy changes in malignant glioma can mimic tumor progression. *Neurology*. 2004;63(3):535-537.
121. Stupp R, Mason WP, van den Bent MJ, et al. Radiotherapy plus concomitant and adjuvant temozolomide for glioblastoma. *N Engl J Med*. 2005;352(10):987-996.
122. Chamberlain MC, Glantz MJ, Chalmers L, Van Horn A, Sloan AE. Early necrosis following concurrent Temodar and radiotherapy in patients with glioblastoma. *J Neurooncol*. 2006;82(1):81-83.
123. Brandsma D, Stalpers L, Taal W, Sminia P, van den Bent MJ. Clinical features, mechanisms, and management of pseudoprogression in malignant gliomas. *Lancet Oncol*. 2008;9(5):453-461.
124. Brandes AA, Franceschi E, Tosoni A, et al. MGMT promoter methylation status can predict the incidence and outcome of pseudoprogression after concomitant radiochemotherapy in newly diagnosed glioblastoma patients. *J Clin Oncol*. 2008;26(13):2192-2197.
125. Taal W, Brandsma D, de Bruin HG, et al. Incidence of early pseudo-progression in a cohort of malignant glioma patients treated with chemoirradiation with temozolomide. *Cancer*. 2008;113(2):405-410.
126. Naftel RP, Pollack IF, Zuccoli G, Deutsch M, Jakacki RI. Pseudoprogression of low-grade gliomas after radiotherapy. *Pediatr Blood Cancer*. 2014;62(1):35-39.
127. Pružincová Ľ, Šteňo J, Srbecký M, et al. MR imaging of late radiation therapy- and chemotherapy-induced injury: a pictorial essay. *Eur Radiol*. 2009;19(11):2716-2727.
128. Mamlouk MD, Handwerker J, Ospina J, Hasso AN. Neuroimaging findings of the post-treatment effects of radiation and chemotherapy of malignant primary glial neoplasms. *Neuroradiol J*. 2013;26(4):396-412.
129. Young RJ, Gupta A, Shah AD, et al. Potential utility of conventional MRI signs in diagnosing pseudoprogression in glioblastoma. *Neurology*. 2011;76(22):1918-1924.
130. Song YS, Choi SH, Park C-K, et al. True progression versus pseudoprogression in the treatment of glioblastomas: a comparison study of normalized cerebral blood volume and apparent diffusion coefficient by histogram analysis. *Korean J Radiol*. 2013;14(4):662-672.
131. Lee WJ, Choi SH, Park C-K, et al. Diffusion-weighted MR imaging for the differentiation of true progression from pseudoprogression following concomitant radiotherapy with temozolomide in patients with newly diagnosed high-grade gliomas. *Acad Radiol*. 2012;19(11):1353-1361.
132. Chu HH, Choi SH, Ryoo I, et al. Differentiation of true progression from pseudoprogression in glioblastoma treated with radiation therapy and concomitant temozolomide: comparison study of standard and high-b-value diffusion-weighted imaging. *Radiology*. 2013;269(3):831-840.
133. Plotkin M, Eisenacher J, Bruhn H, et al. 123I-IMT SPECT and 1H MR-spectroscopy at 3.0 T in the differential diagnosis of recurrent or residual gliomas: a comparative study. *J Neurooncol*. 2004;70(1):49-58.

134. Zhang H, Ma L, Wang Q, Zheng X, Wu C, Xu B-N. Role of magnetic resonance spectroscopy for the differentiation of recurrent glioma from radiation necrosis: a systematic review and meta-analysis. *Eur J Radiol*. 2014;83(12):2181-2189.
135. Shiroishi MS, Boxerman JL, Pope WB. Physiologic MRI for assessment of response to therapy and prognosis in glioblastoma. *Neuro Oncol*. 2016;18(4):467-478.
136. Di Costanzo A, Scarabino T, Trojsi F, et al. Recurrent glioblastoma multiforme versus radiation injury: a multiparametric 3-T MR approach. *Radiol Med*. 2014;119(8):616-624.
137. Matsusue E, Fink JR, Rockhill JK, Ogawa T, Maravilla KR. Distinction between glioma progression and post-radiation change by combined physiologic MR imaging. *Neuroradiology*. 2009;52(4):297-306.
138. Caroline I, Rosenthal MA. Imaging modalities in high-grade gliomas: pseudoprogression, recurrence, or necrosis? *J Clin Neurosci*. 2012;19(5):633-637.
139. Chung WJ, Kim HS, Kim N, Choi CG, Kim SJ. Recurrent glioblastoma: optimum area under the curve method derived from dynamic contrast-enhanced T1-weighted perfusion MR imaging. *Radiology*. 2013;269(2):561-568.
140. Narang J, Jain R, Arbab AS, et al. Differentiating treatment-induced necrosis from recurrent/progressive brain tumor using nonmodel-based semiquantitative indices derived from dynamic contrast-enhanced T1-weighted MR perfusion. *Neuro Oncol*. 2011;13(9):1037-1046.
141. Choi YJ, Kim HS, Jahng G-H, Kim SJ, Suh DC. Pseudoprogression in patients with glioblastoma: added value of arterial spin labeling to dynamic susceptibility contrast perfusion MR imaging. *Acta Radiol*. 2013;54(4):448-454.
142. Yun TJ, Park C-K, Kim TM, et al. Glioblastoma treated with concurrent radiation therapy and temozolomide chemotherapy: differentiation of true progression from pseudoprogression with quantitative dynamic contrast-enhanced MR imaging. *Radiology*. 2015;274(3):830-840.
143. Lotumolo A, Caivano R, Rabasco P, et al. Comparison between magnetic resonance spectroscopy and diffusion weighted imaging in the evaluation of gliomas response after treatment. *Eur J Radiol*. 2015;84(12):2597-2604.
144. Jalbert LE, Neill E, Phillips JJ, et al. Magnetic resonance analysis of malignant transformation in recurrent glioma. *Neuro Oncol*. 2016;18(8):1169-1179.
145. Henry RG, Vigneron DB, Fischbein NJ, et al. Comparison of relative cerebral blood volume and proton spectroscopy in patients with treated gliomas. *Am J Neuroradiol*. 2000;21(2):357-366.
146. Kimura M, da Cruz LCH. Multiparametric MR imaging in the assessment of brain tumors. *Magn Reson Imaging Clin N Am*. 2016;24(1):87-122.
147. Shah AH, Snelling B, Bregy A, et al. Discriminating radiation necrosis from tumor progression in gliomas: a systematic review what is the best imaging modality? *J Neurooncol*. 2013;112(2):141-152.
148. Verma N, Cowperthwaite MC, Burnett MG, Markey MK. Differentiating tumor recurrence from treatment necrosis: a review of neuro-oncologic imaging strategies. *Neuro Oncol*. 2013;15(5):515-534.
149. Batchelor TT, Sorensen AG, di Tomaso E, et al. AZD2171, a pan-VEGF receptor tyrosine kinase inhibitor, normalizes tumor vasculature and alleviates edema in glioblastoma patients. *Cancer Cell*. 2007;11(1):83-95.
150. Hygino da Cruz LC, Rodriguez I, Domingues RC, Gasparetto EL, Sorensen AG. Pseudoprogression and pseudoresponse: imaging challenges in the assessment of posttreatment glioma. *Am J Neuroradiol*. 2011;32(11):1978-1985.
151. Keunen O, Johansson M, Oudin A, et al. Anti-VEGF treatment reduces blood supply and increases tumor cell invasion in glioblastoma. *Proc Natl Acad Sci USA*. 2011;108(9):3749-3754.
152. Nowosielski M, Wiestler B, Goebel G, et al. Progression types after antiangiogenic therapy are related to outcome in recurrent glioblastoma. *Neurology*. 2014;82(19):1684-1692.
153. Boxerman JL, Zhang Z, Safriel Y, et al. Early post-bevacizumab progression on contrast-enhanced MRI as a prognostic marker for overall survival in recurrent glioblastoma: results from the ACRIN 6677/RTOG 0625 Central Reader Study. *Neuro Oncol*. 2013;15(7):945-954.
154. Kothari PD, White NS, Farid N, et al. Longitudinal restriction spectrum imaging is resistant to pseudoresponse in patients with high-grade gliomas treated with bevacizumab. *Am J Neuroradiol*. 2013;34(9):1752-1757.
155. Yamasaki F, Kurisu K, Aoki T, et al. Advantages of high b-value diffusion-weighted imaging to diagnose pseudo-responses in patients with recurrent glioma after bevacizumab treatment. *Eur J Radiol*. 2012;81(10):2805-2810.
156. Rieger J, Bähr O, Müller K, Franz K, Steinbach J, Hattingen E. Bevacizumab-induced diffusion-restricted lesions in malignant glioma patients. *J Neurooncol*. 2010;99(1):49-56.
157. Ratai E-M, Zhang Z, Snyder BS, et al. Magnetic resonance spectroscopy as an early indicator of response to anti-angiogenic therapy in patients with recurrent glioblastoma: RTOG 0625/ACRIN 6677. *Neuro Oncol*. 2013;15(7):936-944.
158. Hattingen E, Bähr O, Rieger J, Blasel S, Steinbach J, Pilatus U. Phospholipid metabolites in recurrent glioblastoma: in vivo markers detect different tumor phenotypes before and under antiangiogenic therapy. *PLoS One*. 2013;8(3):1-10.
159. Stadlbauer A, Pichler P, Karl M, et al. Quantification of serial changes in cerebral blood volume and metabolism in patients with recurrent glioblastoma undergoing antiangiogenic therapy. *Eur J Radiol*. 2015;84(6):1128-1136.
160. Hutterer M, Hattingen E, Palm C, Proescholdt MA, Hau P. Current standards and new concepts in MRI and PET response assessment of antiangiogenic therapies in high-grade glioma patients. *Neuro Oncol*. 2015;17(6):784-800.
161. Yang D. Standardized MRI assessment of high-grade glioma response: a review of the essential elements and pitfalls of the RANO criteria. *Neuro Oncol Pract*. 2015. doi:10.1093/nop/npv023.
162. Linhares P, Carvalho B, Figueiredo R, Reis RM, Vaz R. Early pseudoprogression following chemoradiotherapy in glioblastoma patients: the value of RANO evaluation. *J Oncol*. 2013;2013(5):1-9.
163. Trifiletti DM, Lee C-C, Schlesinger D, Larner JM, Xu Z, Sheehan JP. Leukoencephalopathy after stereotactic radiosurgery for brain metastases. *Int J Radiat Oncol Biol Phys*. 2015;93(4):870-878.
164. Monaco EA, Faraji AH, Berkowitz O, et al. Leukoencephalopathy after whole-brain radiation therapy plus radiosurgery versus radiosurgery alone for metastatic lung cancer. *Cancer*. 2013;119(1):226-232.
165. Rauch PJ, Park HS, Knisely JPS, Chiang VL, Vortmeyer AO. Delayed radiation-induced vasculitic leukoencephalopathy. *Int J Radiat Oncol Biol Phys*. 2012;83(1):369-375.
166. Nagesh V, Tsien CI, Chenevert TL, et al. Radiation-induced changes in normal-appearing white matter in patients with cerebral tumors: a diffusion tensor imaging study. *Int J Radiat Oncol Biol Phys*. 2008;70(4):1002-1010.
167. Rimkus C, de M, Andrade CS, Leite CDC, McKinney AM, Lucato LT. Toxic leukoencephalopathies, including drug, medication, environmental, and radiation-induced encephalopathic syndromes. *Semin Ultrasound CT MR*. 2014;35(2):97-117.
168. Kerklaan JP, Lycklama á Nijeholt GJ, Wiggenraad RGJ, Berghuis B, Postma TJ, Taphoorn MJB. SMART syndrome: a late reversible complication after radiation therapy for brain tumours. *J Neurol*. 2011;258(6):1098-1104.
169. Kleinig TJ. Associations and implications of cerebral microbleeds. *J Clin Neurosci*. 2013;20(7):919-927.
170. Shobha N, Smith EE, Demchuk AM, Weir NU. Small vessel infarcts and microbleeds associated with radiation exposure. *Can J Neurol Sci*. 2009;36(3):376-378.
171. Sakata A, Kanagaki M, Yamamoto A, et al. Radiation-associated tumors in the central nervous system and the head and neck: what radiologists should know. *Neurographics*. 2016;6(2):88-97.
172. Ecemis GC, Atmaca A, Meydan D. Radiation-associated secondary brain tumors after conventional radiotherapy and radiosurgery. *Expert Rev Neurother*. 2013;13(5):557-565.
173. Umansky F, Shoshan Y, Rosenthal G, Fraifeld S, Spektor S. Radiation-induced meningioma. *Neurosurg Focus*. 2008;24:E7. doi:10.3171/FOC/2008/24/5/E7.
174. Morgenstern PF, Shah K, Dunkel IJ, et al. Meningioma after radiotherapy for malignancy. *J Clin Neurosci*. 2016;30:93-97. doi:10.1016/j.jocn.2016.02.002.